CENTER FOR ASTROPHYSICS
HARVARD & SMITHSONIAN

Submillimeter Array Newsletter

Number 37, January 2024

CONTENTS

1 From the Director

SCIENCE HIGHLIGHTS:

2 SMA and JWST Uncover an Ultra-massive z = 4.26 Submillimeter Galaxy that is Invisible to HST

6 SMAPOL: Full-Stokes Polarization Monitoring of AGN jets in the Light of the First X-ray Polarimetric Mission

TECHNICAL HIGHLIGHTS:

10 Checking the Weather: Using Public Forecast Data for SMA Scheduling

13 Here Comes the Sun — Preparing the SMA for Solar Observing

14 New wSMA Cryostats With Enhanced Cooling Power Delivered

OTHER NEWS

16 Call for Proposals

Proposal Statistics

17 Track Allocations

18 Top-Ranked Proposals

19 All SAO Proposals

22 Recent Publications

FROM THE DIRECTOR

Dear SMA Newsletter readers,

The SMA continues to produce significant data resulting in quality papers and garner a great deal of interest. In 2023, proposals were at a 4:1 oversubscription rate. All partner institutions were well represented. Like other observatories, the SMA has had to manage in a difficult current funding environment, and the Hilo and Cambridge technical teams have worked heroically to maintain observing productivity, with at least six antennas available for 86% of operations. Priorities are to maintain operations while investigating enhancements and upgrades such as transporter drive and antenna motor drives.

Strategies for funding major upgrades will be reported as they evolve. Funding smaller projects, such as chopper drive system upgrades, is within current budget constraints and in process.

Development of the wSMA has long been part of the upgrade strategy, not only for increased bandwidth and performance, but to replace systems which are getting more difficult to repair or replace. We are beginning to see the project bear fruit. The prototype wSMA cryostat has been installed in Antenna 7 and two new wSMA cryostats, with enhanced cooling, have been delivered to Cambridge. We anticipate one new wSMA receiver will be ready for shipping to Hawaii in six months, the other by the end of 2024. We plan to initiate procurement of the next two cryostats in Q2 of 2024 using existing funds. As these come online, the old systems become available spares to existing, previous generation, receivers/cryostats.

The Solar SMA project received a boost from internal CfA funds to initiate the investigation into retrofit work necessary to sufficiently protect the antennas from the effects of focused sunlight.

A Smithsonian Scholarly Studies proposal was accepted and fully funded; Reproducible & Accessible Sub-mm Science Tutorials: Unlocking the vast SMA Archive. The class has been, and will continue to be, a factor in the continued growth of SMA use by the science community.

Smithsonian Institution facilities continue to invest in the SMA. Paving at the summit was completed last summer, The new Hilo office generator system is nearing completion. The "Flywheel" generator at the summit has begun. The PACU project at the summit (air conditioning, fire suppression, etc.) is just getting underway. A summit building refurbishment project is on the books and expected to start in 2025. A Hilo office building refurbishment project is in the design phase, likely to start 2026.

In closing, I would like to take this opportunity to remember Jack Barrett, with whom many of you have worked for many years in the Receiver Lab, and George Nystrom, long time SMA friend and engineering colleague. Sadly, we lost both this past year.

Enjoy the remainder of this newsletter as it highlights scientific and technical advancements of the SMA team.

Tim Norton

SMA AND JWST UNCOVER AN ULTRA-MASSIVE Z = 4.26 SUBMILLIMETER GALAXY THAT IS INVISIBLE TO HST

Ian Smail[1], Ugnė Dudzevičiūtė[2], Mark Gurwell[3], Giovanni G. Fazio[3], S.P. Willner[3], Rogier A. Windhorst[4] & the A1489-PEARLS team

Recent claims of the apparently early formation of massive high-redshift galaxies detected by JWST has caused some theoretical consternation (e.g., Labbe et al. 2023). However, this may be simply the latest emergence of some of the same issues with galaxy formation models that have caused them to struggle to reproduce observations of massive dusty star-forming galaxies at $z \geq 1$. Indeed, observations of the distant Universe with JWST are prompting a wider appreciation of the role of dust in defining the observed properties of a wide range of high-redshift galaxy populations (e.g., Barrufet et al. 2023; Bisigello et al. 2023; Kokorev et al. 2023; Magnelli et al. 2023; Perez-Gonzalez et al. 2023).

Obscuration by dust has been known to be a complicating factor in understanding the properties of high-redshift galaxies for the last ~30 years. The first studies of $z > 3$ star-forming galaxies employed samples selected through their rest-frame ultraviolet (UV) emission (e.g., Steidel & Hamilton 1993). However, the subsequent identification in the submillimeter waveband of highly dust-obscured galaxies at similar redshifts (e.g., Ivison et al. 1998) demonstrated the presence of a population of much more active and massive galaxies than those typically detectable in the rest-frame UV (Ivison et al. 2000). The potential significance of such UV/optically-faint galaxy populations was underlined by the analysis of the first large samples of dust-obscured galaxies identified with sub/millimeter interferometers (see Casey et al. 2014; Hodge & da Cunha 2020) including early work with SMA (Younger et al. 2007, 2008, 2009). These studies indicated that dust-obscured galaxies typically have high stellar masses ($M_* \sim 10^{11}$ M_o, e.g., Dudzevičiūtė et al. 2020) and most of the star formation in the Universe at $z < 4–5$ is believed to occur in these obscured systems (Bouwens et al. 2020). Indeed, it was the rapid evolution in this dust-obscured activity that created ``*cosmic noon*'' – the peak in the star-formation rate density at $z \sim 2$ (e.g., Magnelli et al. 2013). Discovering the physical processes driving this dust-obscured population is thus crucial for understanding galaxy evolution.

A recent joint SMA/JWST/HST study (Smail et al. 2023, hereafter S23[5]) has underlined both the importance of dust obscuration in censoring studies of galaxy evolution and the presence of rare massive galaxies at high redshifts. This study focused on two bright submillimeter sources, 850.1 and 850.2, that were serendipitously detected in a shallow archival SCUBA-2 850 μm map of the $z = 0.35$ galaxy cluster Abell 1489. These sources were identified when an assessment was made of the SCUBA-2 coverage of regions scheduled for JWST observations as part of the PEARLS GTO program (Windhorst et al. 2023). Both submillimeter sources were unusually bright, 850.1 and 850.2 having 850-μm flux densities of $S_{850\mu m} \sim$ 50mJy and 20mJy respectively, indicating that they were either strongly gravitationally amplified by the galaxy cluster or intrinsically very luminous.

SMA DDT observations in early 2022 (2021B-072) precisely located both sources and confirmed that the brighter one, 850.1 (Fig. 1), is an intrinsically luminous submillimeter galaxy magnified by ~4× by the foreground cluster and with a lensing-corrected 850-μm flux density of $S_{850\mu m}$~14mJy (such bright sources are very rare with a surface density of just ~10 degree^{-2}), while the fainter source, 850.2, is magnified by ~6×

[1]CEA, Durham University; [2]MPIA, Heidelberg; [3]Center for Astrophysics | Harvard and Smithsonian; [4]SESE, Arizona State University.

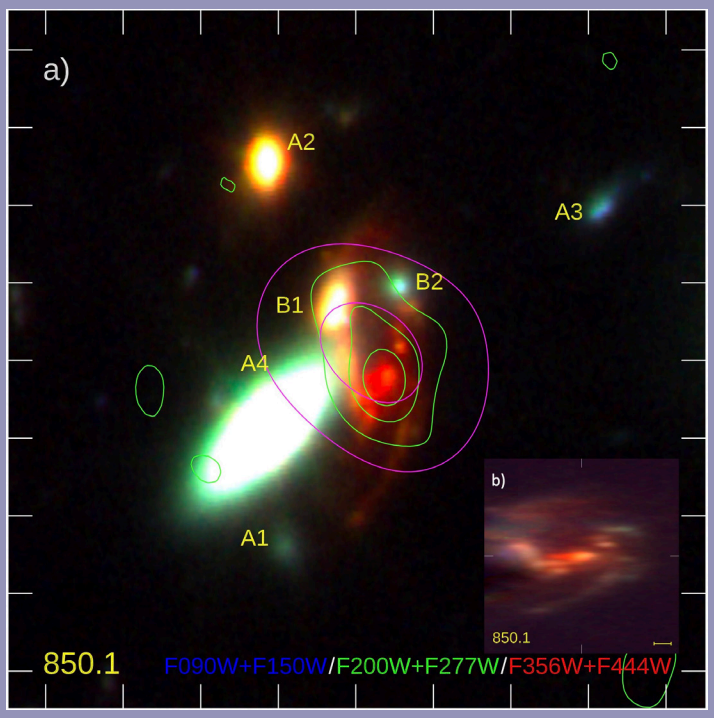

Figure 1: a) Three-color JWST NIRCam image of a 9'' × 9'' region centered on 850.1, the more luminous of the two z=4.26 submillimeter galaxies seen through Abell 1489 from Smail et al. (2023). The image in panel a) is constructed using F090W+F150W as blue, F200W+F277W as green, and F356W+F444W as red. Panel b) shows a 5''×5'' region around 850.1 "de-sheared" to correct for the lensing magnification (the scale bar indicates 1 kpc) using F277W, F356W and F444W. Panel a) also shows the SMA 880-μm contours in green (starting from 2σ in 7-σ increments), which unambiguously identify the submillimeter source. Also shown is the new lower-resolution SMA [CII] detection in magenta. The JWST imaging shows that 850.1 is an extremely red, galaxy with a strong central bar connected to arm-like features and lying close to a bright, foreground disk galaxy (A4) with several fainter galaxies (A2–A4) nearby. 850.1 and the possible companion B2 are both at z=4.26, while all the other features (A1–A4, B1) are believed to lie in the foreground cluster at z~0.35. This figure is adapted from S23.

and is a more typical submillimeter galaxy with an intrinsic flux density of $S_{850\mu m}$~4mJy.

Subsequent NOEMA 3-mm observations and very recent SMA observations (2023B-S039) of these two sources detected CO 5–4, 4–3 and [CI] and [CII] emission lines (Fig. 2), yielding redshifts of z = 4.26 for both galaxies and demonstrating that they reside in a single group-like structure (they are separated on the sky by ~100 kpc in the source plane). Deeper SCUBA-2 observations also uncovered a third bright submillimeter source, 850.3, around ~2′ away, outside the sensitive region of the original SMA/NOEMA coverage. Again, our recent SMA observations have now provided a firm identification for this submillimeter source, the IRAC colors of which strongly suggest that it also lies at z ~ 4 and so may reside in the same high-redshift structure.

With the precise location for the two galaxies from SMA, S23 could exploit the 9-band JWST and HST imaging to study the stellar structure of these systems. The first striking discovery was that 850.1 is very red and effectively invisible shortward of ~2μm (Fig. 3), undetected in either HST or the bluer near-infrared JWST filters. Corrected for lens amplification 850.1 has near-infrared magnitudes of H ~ 29 and K ~ 27. Thus, neither HST nor ground-based K-band surveys would have been able to detect this class of source, let alone less-massive or higher-redshift examples.

The thermal infrared coverage of JWST also showed evidence for a bar-like stellar feature in the central regions of 850.1 (Fig. 1 & 3), one of the highest redshift examples known. If such a bar is also present in the galaxy's gas distribution, then the radial inflow of gas may explain the high star-formation rate, ~1,000 $M_\odot$ yr^{-1}, seen in this galaxy.

Using the multi-band JWST+HST imaging S23 then analysed the internal structure of 850.1 and 850.2 by modelling the spectral energy distributions (SED) of the sources at 0.18″ (~1kpc) resolution (Fig. 3). This pixel-level SED analysis included the essential SMA 880μm maps necessary to constrain the dust-reprocessed emission in these obscured systems. This analysis showed that the lack of emission at <2μm from 850.1 is due to the strong dust reddening, A_V ~ 3–6, over the full ~7 kpc extent of the system (Fig. 3). Critically, the high-resolution JWST imaging could also exclude significant contamination from obscured AGN in the SED analysis, and S23 inferred a very high stellar mass density core within the central regions of 850.1, the presence of which may be linked to the quenching of star formation and the modest gas fraction in this system. This analysis indicates that 850.1 is a one of the most massive galaxies known at z > 4, with a stellar mass of ~6 × $10^{11} M_\odot$ and a total baryonic mass at ~$10^{11.8} M_\odot$. Nevertheless, with an estimated a space density of ~3 × 10^{-7} Mpc^{-3}, the galaxy is consistent with the expected numbers of high-mass, high-redshift systems in a ΛCDM model.

The high mass estimated for 850.1 suggests it is likely to be the central galaxy of the group it inhabits, with 850.2 a much lower mass companion (as well as potentially the recently located 850.3). This discovery adds to the growing evidence suggesting that submillimeter galaxies represent maximally efficient galaxy formation occurring in group-like environ-

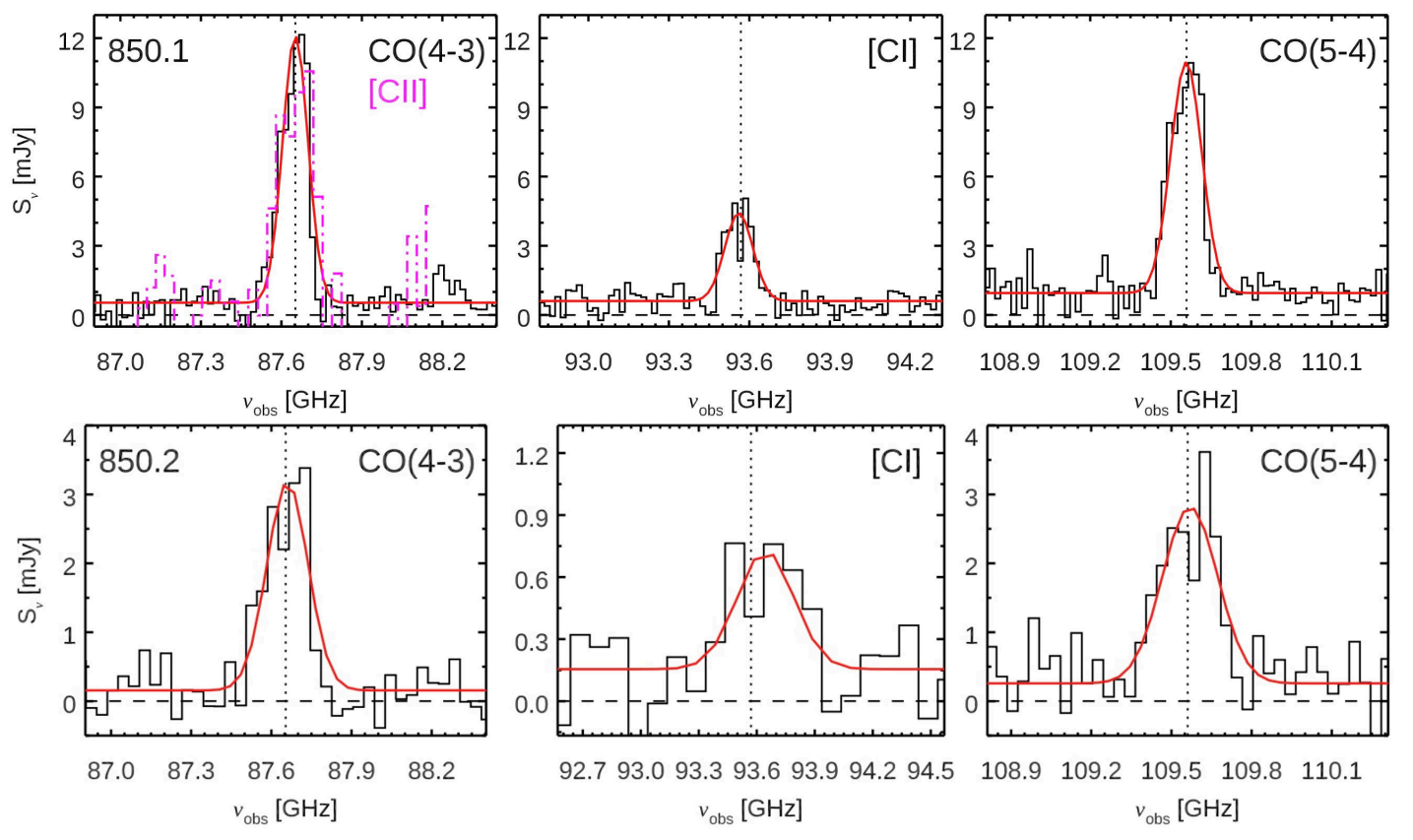

Figure 2: NOEMA 3 mm spectra for 850.1 (top) and 850.2 (bottom), showing the CO(4–3), [C I](1–0), and CO(5–4) emission lines, as well as the SMA detection of [CII] in 850.1 from 2023B.S039 (overplotted in the top-left panel, scaled to the CO(4–3) peak). The panels are centered on the expected frequencies of the lines at the adopted redshifts for each source and a model fit comprising a Gaussian and a constant continuum level is shown for each line. Both sources have relatively weak [C I] emission compared to their CO(4–3) and CO(5–4), suggesting a relatively modest characteristic ISM density of Log(n)~4.5cm^{-3}. This figure is adapted from S23.

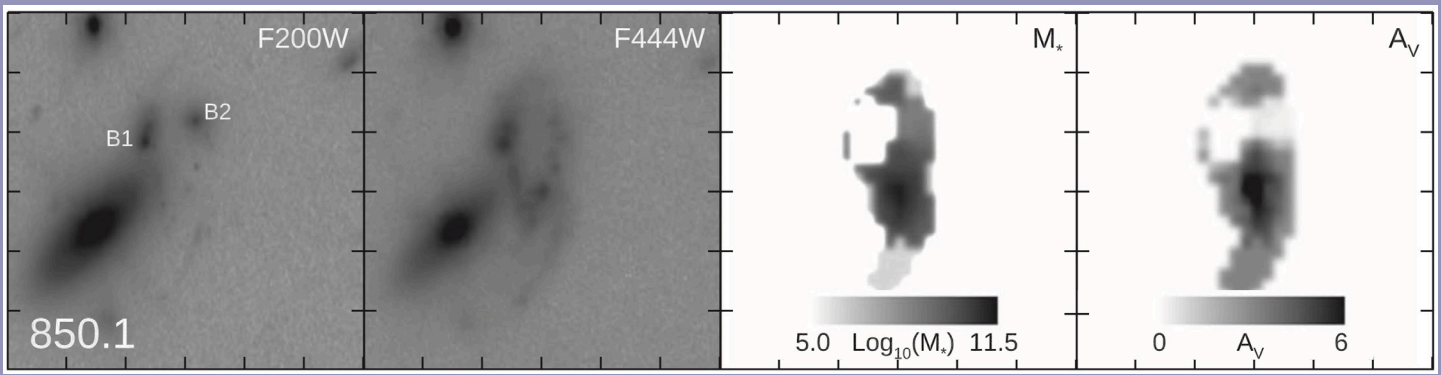

Figure 3: 6'' × 6'' thumbnails of 850.1 showing the JWST NIRCam F200W and F444W images, illustrating the faintness of the galaxy in the F200W filter, along with the maps of the stellar mass and A_V on <1kpc scales in the galaxy. The stellar-mass surface density is per ~0.6 × 0.6 kpc pixel in the source plane. These maps show the very high stellar mass densities and reddening seen in the central regions of 850.1. The blue source B1 is excluded from the analysis due to the poor quality of the SED fits at z = 4.26, supporting its likely lower redshift. While B2 has much lower A_V and stellar-mass surface density compared to the bulk of 850.1, suggesting that it may be a companion galaxy. This figure is adapted from S23.

ments at high redshifts (e.g., Stach et al. 2021). The strong gravitational torques expected from the frequent interactions between galaxies in such environments may prompt the formation of bars which combined with their high gas mass fractions could be the fundamental explanation for the vigorous activity seen in the submillimeter population and its strong evolution with redshift (e.g., Dudzevičiūtė et al. 2020). This is in turn could be the missing element of theoretical models needed to match the rapid formation of massive galaxies at high redshifts (Fragkoudi et al. 2021).

Without the lensing effect of the foreground cluster, 850.1 and 850.2 would appear as a single, blended, bright ($S_{850\mu m}$ ~17 mJy) source in a single-dish submillimeter survey. There are several similar lensed groups at $z \sim 2–4$, comprising one or more dusty star-forming galaxies and other companions, reported in the literature. The frequency with which these systems are being found may reflect the correspondence between the spatial scale of group-sized halos and the size of high-magnification region of massive galaxy clusters at $z \leq 1$. This adds evidence that at least a subset of the high-redshift submillimeter population resides in group-scale halos. These are expected to be the most active environments for the accretion of both companion galaxies and gas from the surrounding intergalactic medium, potentially providing both the trigger and the fuel needed to power their active star formation.

In conclusion, SMA's identification of a pair of bright SMGs, 850.1 and 850.2, seen through the core of Abell 1489 illustrates the remarkable diversity of galaxies hosting massive dust and gas reservoirs at high redshifts. These two galaxies are associated with a single structure at $z = 4.26$, but their observed and intrinsic properties span the full range known for this population at $z > 4$. The structure of 850.1 is particularly noteworthy, with features that appear to correspond to arms and a central bar in a very massive galaxy at $z = 4.26$. It is tempting to identify these features as a response to dynamical perturbations from the group environment, including the presence of 850.2 (and potentially 850.3) as a close companion. The bar has a similar size to the dust continuum peak and the massive stellar core in 850.1, suggesting that this galaxy is experiencing a bar-driven inflow that is fueling a central starburst in its baryon-dominated core. The study of high-redshift dusty star-forming galaxies with SMA and JWST/NIRCam within the PEARLS survey will be expanded beyond these two bright lensed examples to the more typical examples of the population at millijansky-flux levels with the ongoing SMA+JWST survey of the PEARLS Time Domain Field at the North Ecliptic Pole, which has been imaged with SCUBA-2 by Hyun et al. (2023).

REFERENCES

- Barrufet, L., et al., 2023, MNRAS, 522, 449
- Bisigello, L., et al., 2023, A&A, 676, 76
- Bouwens, R., et al., 2020, ApJ, 902, 112
- Casey, C.M., et al., 2014, PhR, 541, 45
- Dudzevičiūtė, U., et al., 2020, MNRAS, 494, 3828
- Hodge, J., da Cunha, E., 2020, RSOS, 7, 200556
- Hyun, M., et al., 2023, ApJS, 264, 19
- Fragkoudi, F., et al., 2021, A&A, 650, L16
- Ivison, R.J., et al., 1998, MNRAS, 298, 583
- Ivison, R.J., et al., 2000, MNRAS, 315, 209
- Kokorev, C., et al., 2023, ApJ, 945, L24
- Labbe, I., et al., 2023, Nature, 616, 266
- Magnelli, B., et al., 2013, A&A, 553, 132
- Magnelli, B., et al., 2023, A&A, 678, A83
- Perez-Gonzalez, P.G., et al., 2023, ApJ, 946, L16
- Smail, I., et al., 2023, ApJ, 958, 36 [S23]
- Stach, S.M., et al., 2021, MNRAS, 504, 172
- Steidel, C.C., Hamilton, D., 1993, ApJ, 105, 2017
- Windhorst. R.A., et al. 2023, AJ, 165, 13
- Younger, J.D., et al., 2007, ApJ, 671, 1241
- Younger, J.D., et al., 2008, ApJ, 688, 59
- Younger, J.D., et al., 2009, ApJ, 704, 803

SMAPOL: FULL-STOKES POLARIZATION MONITORING OF AGN JETS IN THE LIGHT OF THE FIRST X-RAY POLARIMETRIC MISSION

Ioannis Myserlis[1,2], Ramprasad Rao[3], Mark Gurwell[3], Garrett Keating[3], Ivan Agudo[4], Alan Marscher[5], Svetlana Jorstad[5,6], Clemens Thum[1], Giacomo Bonnoli[7]

Jets from Active galactic nuclei (AGN) comprise the most energetic, persistent phenomenon in the Universe. Manifested as collimated beams of relativistic magnetized plasma, AGN jets are thought to be propelled and focused by helical magnetic fields and they transport energy and angular momentum through accretion onto supermassive black holes from the central regions of AGN up to distances much larger than the host galaxy, even > 1 Mpc (e.g., Blandford & Znajek 1977; McKinney & Narayan 2007; Tchekhovskoy et al. 2011). Blazars, the subset of jetted AGN where the jet axes are closely aligned to our line of sight ($\lesssim 5^{o}$) are dominated by highly beamed nonthermal emission that is extremely variable (e.g. Marscher 2006), with frequent strong flaring events that vary on timescales of the order of a few weeks at mm wavelengths.

Blazar emission is characterized by an extremely broad spectral range, extending from radio wavelengths to the highest γ-ray energies. Moreover, it has been argued that the brightest

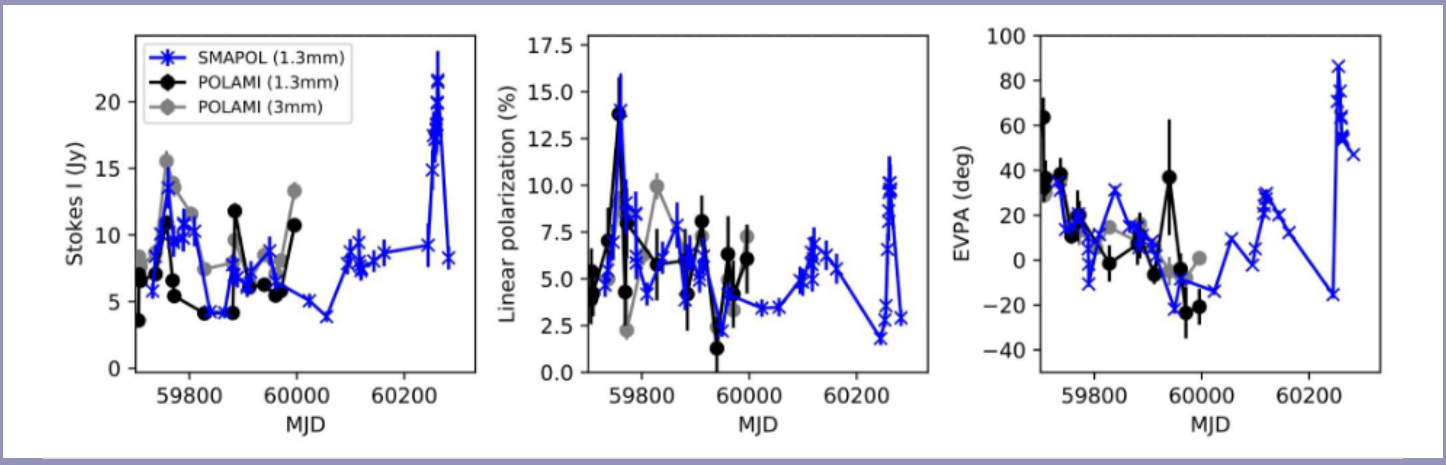

Figure 1: From left to right: Total flux density, linear polarization degree and angle data of BL Lac from SMAPOL (blue x's) and POLAMI (black o's) at 230 GHz (POLAMI data at 3 mm/86 GHz are also shown as grey o's). Rapid LP degree variations and both CW and CCW angle rotations were detected within the first 18 months of SMAPOL observations, consistent with the emitting region being located in compact regions threaded with strong magnetic fields in the acceleration/collimation zone of AGN jets.

[1]Institut de Radioastronomie Millimétrique (IRAM); [2]Max-Planck-Institut für Radioastronomie; [3]Center for Astrophysics | Harvard & Smithsonian; [4]Instituto de Astrofísica de Andalucía-CSIC; [5]Institute for Astrophysical Research, Boston University; [6]Astronomical Institute, St. Petersburg State University; [7]INAF - Brera Astronomical Observatory

blazars produce at least some of the high-energy, astrophysical neutrinos detected by IceCube (e.g. Plavin et al. 2021). The broadband spectrum of blazars can be divided into two main components: the low-frequency component, which is thought to be generated by incoherent synchrotron emission within the jet and spans from radio to optical, UV or even X-rays and, above that range, the high-frequency component, which extends up to the highest γ-ray energies. The emission mechanism of the high-frequency component is currently debated between leptonic and hadronic processes, e.g. inverse-Compton or synchrotron emission through the relativistic electrons or protons that populate the jet, respectively.

Given the remarkably broad spectral range that characterizes their emission and the dependence of synchrotron radiation on the magnetic field, blazars are best studied by the analysis of multiwavelength measurements involving polarimetry, as well as ultra-high-resolution VLBI imaging to help resolve the jet structure. Recently, the first ever X-ray (linear) polarimetry space mission (IXPE) capable of observing weaker X-ray polarimetric sources than the Crab Nebula was launched, Cherenkov Telescope Arrays (e.g. MAGIC) can now reach high sensitivities by means of improved hardware, observational strategies and analysis methods, and multi-messenger astronomy of blazars has been expanded with the IceCube neutrino telescope. Combined with the improved polarimetric analyses of single-dish and interferometric datasets compiled through long term radio monitoring programs at mm and cm wavelengths, such as POLAMI (IRAM 30m telescope), QUIVER (Effelsberg 100m telescope), BEAM-ME or MOJAVE (VLBA), all these advances have opened new windows for relativistic jet studies (e.g. Agudo et al. 2018a;b ; Thum et al. 2018; Myserlis et al. 2018a; Jorstad et al. 2017; Weaver et al. 2022; Lister et al. 2018; Pushkarev et al. 2023).

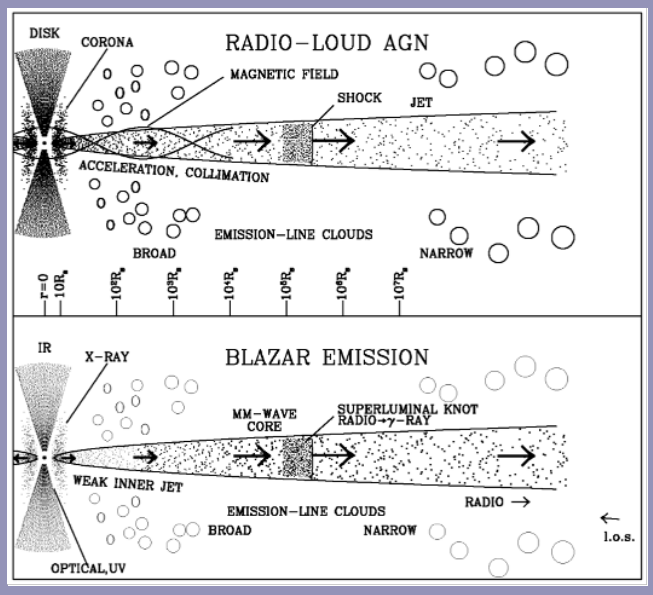

Figure 2: Sketch of a blazar with the various physical components that have either been observed directly or strongly inferred from interpretation of data. Reproduced from Marscher (2006)

SMAPOL (SMA Monitoring of AGNs with POLarization) is a polarization monitoring program that we initiated in June 2022. We perform regular, full polarimetric (Stokes *I, Q, U,* and *V*) observations using SMA at 1.3 mm (230 GHz) every ~2 weeks for a sample of 40 bright AGN jets that have shown increased linear and circular polarization in the past and demonstrate prominent high-energy activity. In addition, as one of the multiwavelength polarimetric monitoring programs that participates in the IXPE Science Team, we perform more dense, coordinated observations whenever the IXPE satellite is pointing at a given blazar, most of which are already included in our sample. Given the high brightness of the SMAPOL targets and the fact that they are unresolved at any SMA array configuration, our observational strategy is highly flexible and maximizes the possibility of obtaining usable data even under adverse observing conditions (even up to 6 mm pwv or as few as four antennas available). Short-term flux variability is also not a significant drawback, since we aim to measure the average polarization of each target over a given track.

The SMA polarimetry system has been extensively used to map the polarization from a wide variety of astrophysical targets including star formation as well as low luminosity AGNs such as SgrA* and M87 (Marrone & Rao 2008, Marrone et al. 2006). The SMAPOL program can deliver high-quality polarimetric measurements at 230 GHz, with a median uncertainty of 0.2% and 2º for the linear polarization degree and angle, respectively. Sample SMAPOL linear polarization degree and angle measurements are shown in Fig. 1 along with POLAMI data at the same frequency using the IRAM 30m telescope, demonstrating the good agreement between the two datasets. It is also evident that SMAPOL data yield smaller uncertainties than POLAMI, mainly because of atmospheric stability and polarimetric bandwidth at 230 GHz (POLAMI measurements are optimized for observations at 3 mm/86 GHz, which show much smaller uncertainties, Fig. 1). The high accuracy and precision of polarimetric calibration in SMA is demonstrated and regularly recorded through our SMAPOL observations, which can be of further use to additional SMA programs.

The radio emission of AGN jets at mm wavelengths is able to overcome the opacity barrier of their innermost regions. As shown in Fig. 2, according to the current physical picture, this region is often populated by relativistic shock fronts, manifested as "knots" in VLBI images that appear to move down the jet at superluminal velocities. Therefore, the high-sensitivity polarization data of the SMAPOL monitoring program trace the

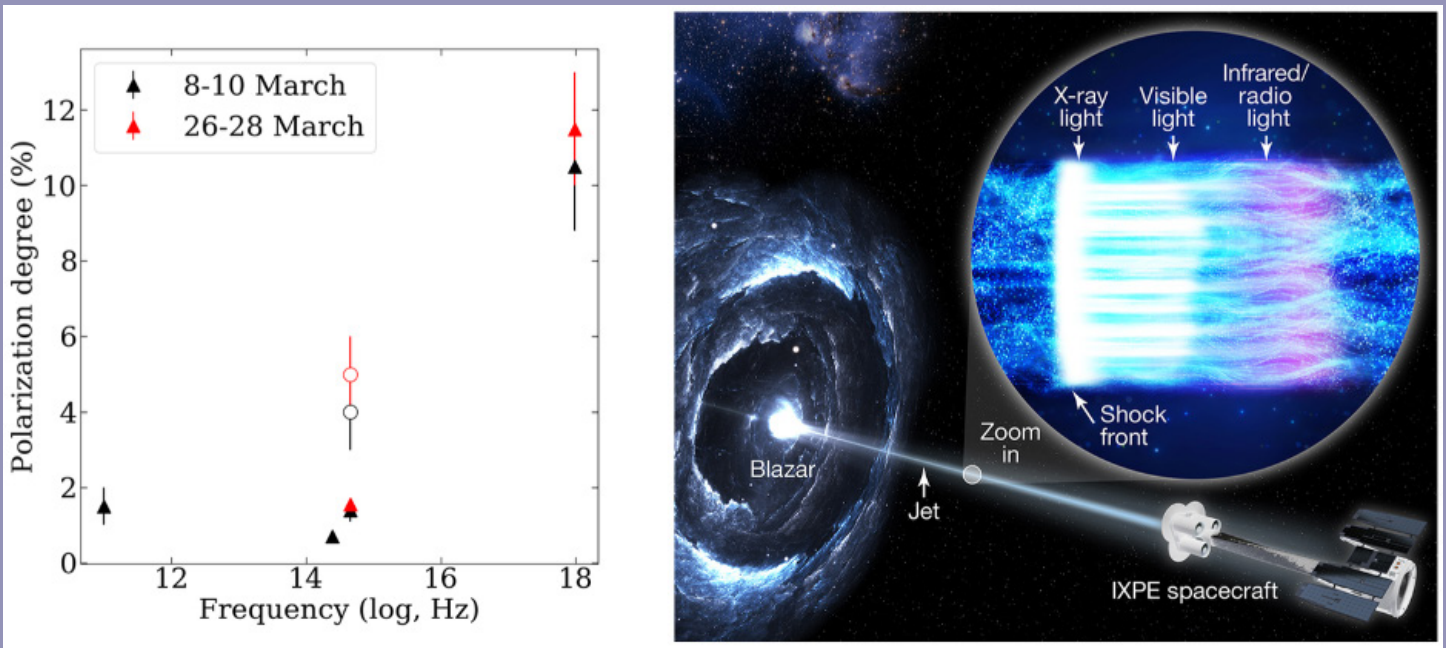

Figure 3: Left panel: Concurrent mm-wave, optical and X-ray polarimetric observations of Mrk 501 (Liodakis et al. 2022). The open symbols show intrinsic optical polarization degree after correcting for the host-galaxy contribution. The strongly chromatic polarization degree, combined with the stable polarization angle across bands (not shown here), suggests that they correspond to synchrotron emission from a shock-accelerated, energy-stratified electron population (right panel, image credit: NASA/Pablo Garcia). At increasing frequencies the emission originates at smaller regions around the shock front, where the magnetic field structure is more ordered.

physical conditions in the vicinity of the central supermassive black hole as well as their evolution as shocks move downstream, which makes them essential in the field.

With SMAPOL, we capitalize on the unprecedented current opportunity to obtain coordinated observations between cm-wave, mm-wave, optical and X-ray (IXPE) polarization. Such concurrent, multi-band polarization data can distinguish between polarized emission from leptonic (i.e. e^- or $e^- - e^+$) and hadronic (i.e. proton-initiated) emission processes, with hadronic models predicting much higher linear polarization degree than leptonic ones (e.g. Zhang & Böttcher 2013). Moreover, overlapping dense polarization monitoring data at cm, mm, optical, and X-ray frequencies can help trace the magnetic field pattern from parsec scales down to the inner regions surrounding the black hole, where higher frequency/energy emission is thought to arise, as newly emerging shock fronts travel down the jet (e.g. Myserlis et al. 2018b).

The role of SMAPOL becomes especially prominent when it comes to the combined analysis of multiwavelength polarization data obtained during extended pointings of the IXPE satellite on selected blazars. In several cases, sources were found to have similar polarization angle but an increasing linear polarization degree throughout mm, optical and X-ray wavelengths, suggesting synchrotron emission in all bands from a shock-accelerated, energy-stratified electron population (e.g. Liodakis et al. 2022; Angelakis et al. 2016). In this scenario, higher energy emission is emerging from more compact regions with well-ordered magnetic field structure in the vicinity of the shock front, as shown in Fig. 3. In other occasions, SMAPOL has observed a higher polarization degree than IXPE, which favors the synchrotron self-Compton mechanism for the jet high-energy emission (e.g. Peirson et al. 2023). In one case, the multiwavelength polarimetric analysis, including SMAPOL data, revealed a helical magnetic field structure in the jet of Mrk 421 (Di Gesu et al. 2023).

To maximize the impact of concurrent, multi-band polarization observations of AGN jets, we aim to continue SMAPOL for the remainder of the IXPE satellite lifespan (recently extended by NASA through September 2025). Having established that significant polarization is often observed across several bands, one of the primary future milestones is to identify polarization degree and angle variations/rotations and investigate their multiwavelength evolution. Such observations will reveal the connection of independent emission regions within AGN jets and trace their physical conditions on much larger scales.

REFERENCES

- Anderson, J. M., Li, Z.-Y., Krasnopolsky, R., & Blandford, R. D. 2003, ApJL, 590, L107
- Bachiller, R. 1996, ARA&A, 34, 111
- Blandford, R. D., & Payne, D. G. 1982, MNRAS, 199, 883
- Hildebrand, R. H. 1983, QJRAS, 24, 267
- Launhardt, R., Pavlyuchenkov, Y., Gueth, F., et al. 2009, A&A, 494, 147
- López-Vázquez, J. A., Cantó, J., & Lizano, S. 2019, ApJ, 879, 42
- Pety, J., Gueth, F., Guilloteau, S., et al. 2006, A&A, 458, 841
- Agudo, I., Thum, C., Molina, S. N., et al. 2018a, MNRAS, 474, 1427
- Agudo, I., Thum, C., Ramakrishnan, V., et al. 2018b, MNRAS, 473, 1850
- Angelakis, E., Hovatta, T., Blinov, D., et al. 2016, MNRAS, 463, 3365
- Blandford, R. D., & Znajek, R. 1977, MNRAS, 179, 433
- Di Gesu, L., Marshall, H. L., Ehlert, S. R., et al. 2023, Nature Astronomy, 7, 1245
- Jorstad, S. G., Marscher, A. P., Morozova, D. A., et al. 2017, ApJ, 846, 98
- Liodakis, I., Marscher, A. P., Agudo, I., et al. 2022, Nature, 611, 677
- Lister, M. L., Aller, M. F., Aller, H. D., et al. 2018, ApJS, 234, 12
- Marrone, D. P., Moran, J. M., Zhao, J.-H., et al. 2006, ApJ, 640, 308
- Marrone, D. P. & Rao, R. 2008, Proceedings of the SPIE, 7020, 70202B
- Marscher, A. P. 2006, ChJAS, 6, 262
- McKinney, J. C, & Narayan, R. 2007, MNRAS, 375, 513
- Myserlis, I., Angelakis, E., Kraus, A., et al. 2018a, A&A, 609, A68
- Myserlis, I., Komossa, S., Angelakis, E., et al. 2018b, A&A, 619, A88
- Peirson, A. L., Negro, M., Liodakis, I., et al. 2023, ApJL, 948, L25
- Plavin, A. V., Kovalev, Y. Y., Kovalev, Y. A., et al. 2021, ApJ, 908, 157
- Pushkarev, A. B., Aller, H. D., Aller, M. F., et al. 2023, MNRAS, 520, 6053
- Tchekhovskoy, A., Narayan, R., & McKinney, J. C. 2011, MNRAS, 418, L79
- Thum, C., Agudo, I., Molina, S. N., et al. 2018, MNRAS, 473, 2506
- Weaver, Z. R., Jorstad, S. G., Marscher, A. P., et al. 2022, ApJS, 260, 12
- Zhang, H. & Böttcher, M. 2013, ApJ, 774, 18

CHECKING THE WEATHER: USING PUBLIC FORECAST DATA FOR SMA SCHEDULING

Scott Paine[1], Ramprasad Rao[1], and Garrett Keating[1]

Numerical weather prediction (NWP) has advanced dramatically over the last four decades, and continues to do so. An engrossing 2015 review in Nature [1] noted that medium-term (3-10 day) forecast skill was improving by about one day per decade, driven by progress in numerical modeling, data assimilation methods, and the density and quality of observations. These improvements create enormous public safety and economic benefits, by supporting preparation for and response to severe weather, and optimization of weather-sensitive activities. [2]

The SMA is one such beneficiary of these improved forecasts. Since 2019, the SMA has been optimizing observations using a planning tool driven by the US Global Forecast System (GFS). The GFS, a coupled land-ocean-atmosphere model produced by the National Centers for Environmental Prediction (NCEP) of the National Oceanic and Atmospheric Administration (NOAA), is the United States' primary global-scale operational NWP system. [3] A 16-day GFS forecast is run four times daily, producing spatiotemporal fields for atmospheric state variables such as wind, temperature, and moisture. For distribution to users, these fields are resampled from their arcane model coordinates to practical latitude and longitude grids down to 0.25 degree resolution; standard vertical pressure coordinates; and temporal steps of 1 hour for the first 5 days and 3 hours thereafter. Remarkably, the GFS operational forecast data are made available to users worldwide at no cost.

The most important meteorological factor governing submillimeter observations (barring inclement weather) is the varying atmospheric opacity caused by changes in atmospheric moisture. The opacity is a spectral quantity, but at a given observing site the opacity at a single reference frequency is an accurate estimator of the opacity over a range of observing frequencies. For millimeter/submillimeter radio observatories at high, dry sites, the established convention is to use the zenith opacity at 225 GHz, known as τ_{225}. (The definition of the opacity or optical depth τ is that the corresponding atmospheric transmittance is $e^{-\tau}$.) Observatories are equipped with tipping radiometers that continuously measure τ_{225}, allowing observers to monitor conditions in real time.

For optimal planning of observations at various frequencies having different requirements on atmospheric opacity, what is needed is a forecast of τ_{225}. The SMA planning tool `sma-met-forecast` provides this information. Every six hours when the latest GFS forecast becomes available, it downloads the 16-day forecast data for temperature, relative humidity, cloud liquid water and ice, ozone, and pressure level heights for a subset of grid points encompassing the SMA. For each forecast time step, these fields are bilinearly interpolated horizontally to the observatory latitude and longitude, and interpolated and truncated vertically at the observatory altitude. The resulting sequence of atmospheric states is then processed using the `am` radiative transfer program [4] to compute τ_{225} as well as integrated column densities for moisture and ozone.

The results are presented in graphical form as shown in Figure 1. The τ_{225} forecast is presented in the top panel, with the most recent forecast shown in black, and the prior 48 hours forecasts shown in light grey. These prior forecasts serve as a "time lag ensemble" helping the user to gauge the accuracy and stability of the forecast. Below the top panel, the forecast zenith column densities for precipitable water vapor

[1]Center for Astrophysics | Harvard and Smithsonian

(PWV), cloud liquid, and cloud ice allow the user to distinguish clear-sky from cloudy conditions. Under clear conditions, PWV also serves as an approximate and familiar proxy for τ_{225}. Finally, the bottom panel tracks ozone–of interest to submillimeter astronomers because of the numerous strong rotational lines of ozone that appear throughout the submillimeter bands.

We have accumulated nearly five years experience with `sma-met-forecast`, including more than four years since the GFS was upgraded to its current FV3 core model in June 2019. [5] Figure 2 shows an assessment of the forecast performance since that time, using τ_{225} measured by the SMA's 225 GHz tipper, a venerable instrument originally deployed on MaunaKea by the Caltech Submillimeter Observatory.

The scatter plot in the top panel compares the hourly median tipper measurements with τ_{225} derived from the GFS analysis. The "analysis" is the initial best-guess atmospheric state that starts off a given forecast run, and is the product of prior forecast states combined with data from surface, upper air, and satellite measurements in a statistical assimilation pro-

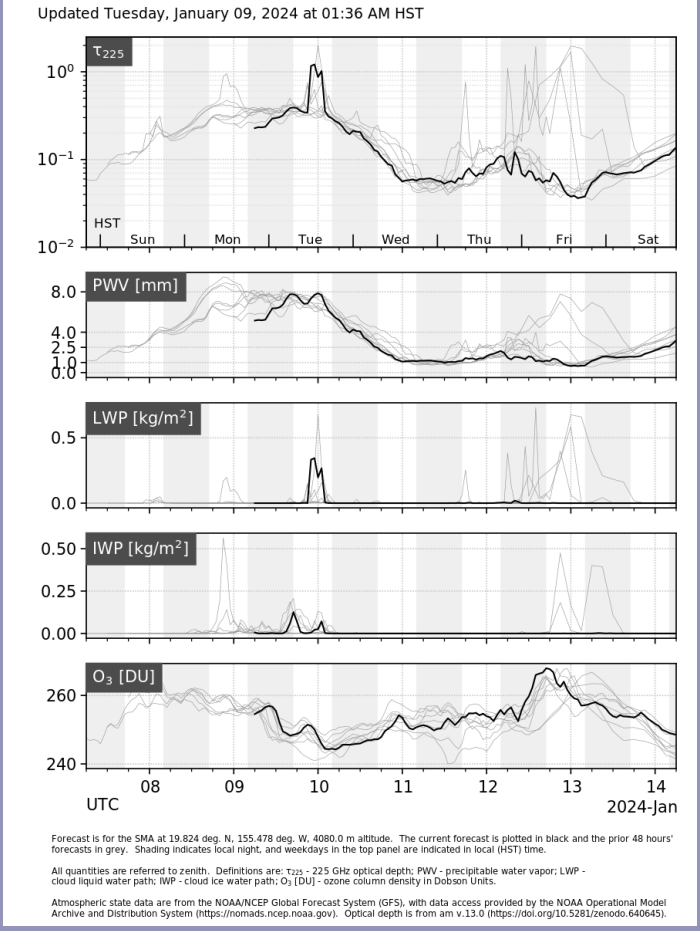

Figure 1: Five-day plot of the output of `sma-met-forecast`. The most recent forecast is shown as a dark trace, and the prior 48 hour's forecasts are shown in light grey. The latter serve as a time-lag ensemble that helps the user assess the forecast uncertainty. For ease of use by observers, both local time (top panel and day/night shading) as well as UTC (bottom panel) are indicated. A similar plot is produced for the full 16-day forecast.

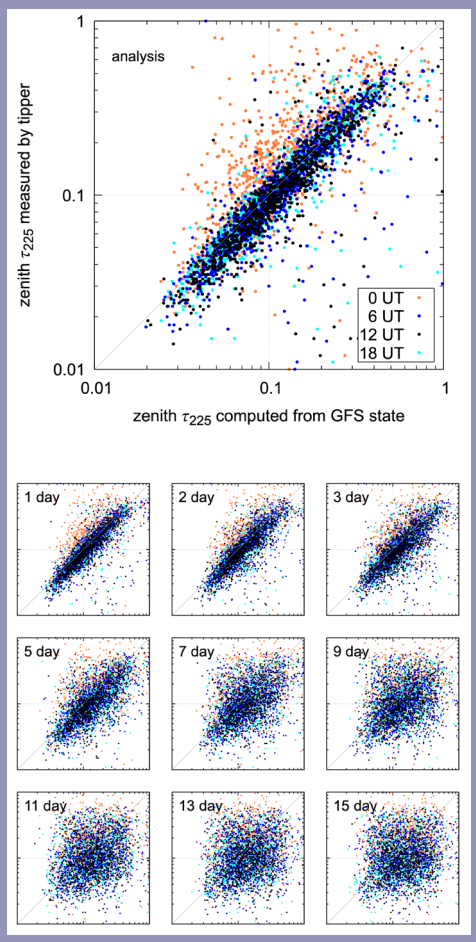

Figure 2: Scatter plots comparing the τ_{225} forecast relative to hourly median measurements from the on-site 225 GHz tipping radiometer. Orange, dark blue, black, and cyan points correspond to UTC (HST) times of 0:00 (2 PM), 6:00 (8 PM), 12:00 (2 AM), and 18:00 (8 AM), respectively. The large top panel compares the tipper measurements with the GFS analysis: this is the initial forecast model state produced by the measurement data assimilation process. As noted in the text, calibration is good with the exception of daytime (orange) data affected by unresolved clouds. The lower panels, on the same axes as the top panel, compare forecasts for increasing time into the future with the tipper measurements as actually occurred, showing the expected progressive decorrelation but with useful skill remaining up to about a week into the future.

cess. It is produced at the four standard synoptic times of 0:00, 6:00, 12:00, and 18:00 UT, corresponding to the orange, dark blue, black, and cyan points respectively. Hawaii is 10 hours behind UT, so the dark blue, black, and cyan points cover 8 PM through 8 AM, roughly the core SMA observing time. The orange points are 2:00 PM in the mid-afternoon.

In general the model and tipper show tight agreement, particularly at night. Moreover, it should be noted that some of the tipper data are spurious, affected by factors such as ice or condensation on the tipper mirror, or instrument malfunctions. In particular, readings below τ_{225}=0.02 are below the dry-air limit for MaunaKea. Also noteworthy are the numerous orange afternoon points indicating tipper measurements exceeding the model. These are unsurprising–the typical afternoon clouds that rise to the summit of MaunaKea are not resolved by the GFS model, which parametrizes clouds at its ~13 km horizontal grid resolution.

The lower nine panels in Figure 2 indicate forecast skill over time. In each of these plots, the horizontal axis is τ_{225} computed from the GFS forecast produced at the indicated time in the past, and the vertical axis is the tipper measurement of τ_{225} as it actually happened. Bearing in mind that the black (2:00 AM local time) points are the ones that matter most, it is clear that detailed observing plans can be supported 3-5 days in advance, and a useful prognosis can be made as much as a week ahead.

The SMA track allocations have three ranges based on the PWV – better than 1 mm, between 1 - 2.5 mm, and between 2.5 - 4 mm. Typically observations made with PWV > 4 mm are considered to be unsatisfactory, though there are situations such as monitoring, for example, where tracks could be run with larger PWV. When the expected PWV is better than 2.5 mm, tracks using frequencies in the 345 GHz band are scheduled, while the 2.5 mm to 4 mm PWV range is reserved for the 230 GHz band observations. There are some situations when a 230 GHz band track could be run at PWV below 2.5 mm in order to take advantage of the somewhat increased sensitivity.

Prior to the use of the GFS forecasts at the SMA (i.e. before 2019), the schedule was primarily driven by the forecasts of the PWV produced by the Maunakea Weather Center (MKWC). These models were fairly coarse in time – 6 hour intervals for 1-3 days and 12 hour intervals from 3-5 days. The MKWC forecast is typically released twice a day on weekdays and no new forecasts are available on weekends and on holidays.

The SMA observations are scheduled dynamically on a daily basis every weekday. The schedule that is created on Friday normally runs through all of the weekend. On longer holiday weekends, the schedule would be made up to 4 days in advance. One of the limitations of the MKWC forecast was the relatively lower time resolution, especially beyond day 3. In addition, the forecasted PWV would start to depart from the measured output, again beyond day 3. As mentioned earlier, the automated GFS forecasts are updated four times every single day. This allows the SMA observation schedules to be changed taking into account the changing predictions. This allows for highly efficient scheduling especially on weekends both regular and long.

For an interferometer such as the SMA, besides atmospheric transmission the stability of the atmospheric phase delays along each antenna's line-of-sight is also of high importance, since differential atmospheric delay fluctuations between antennas reduce coherence of the correlated astronomical signal. For now, `sma-met-forecast` offers no guidance on phase stability, though it is possible that a combination of model fields including wind shear and moisture could be used to derive such a forecast.

The `sma-met-forecast` scripts are easily adaptable to any site, and available to the community on github at **https://github.com/Smithsonian/sma-met-forecast.**

REFERENCES

- Bauer, P., Thorpe, A. & Brunet, G. The quiet revolution of numerical weather prediction. Nature 525, 47–55 (2015). https://doi.org/10.1038/nature14956
- NOAA, 2018, NOAA's Contribution to the Economy; Powering America's Economy and Protecting Americans, https://www.noaa.gov/sites/default/files/legacy/document/2019/Nov/NOAA-Contribution-to-the-Economy-Final.pdf.
- NOAA, GFS, https://www.emc.ncep.noaa.gov/emc/pages/numerical_forecast_systems/gfs.php.
- Paine, Scott. "The am Atmospheric Model" SMA Technical Memo 152. Zenodo, September 19, 2023. https://doi.org/10.5281/zenodo.640645.
- NOAA Geophysical Fluid Dynamics Laboratory. "FV3: Finite-Volume Cubed-Sphere Dynamical Core." https://www.gfdl.noaa.gov/fv3/.

HERE COMES THE SUN — PREPARING THE SMA FOR SOLAR OBSERVING

Garrett Keating[1], on behalf of the *Solar SMA* Team

Over the last 18 months, a group of scientists and engineers — including members from the CE, HEA, R&G, and SSP Divisions of the Center for Astrophysics, as well as member of the US solar science community — have undertaken an effort to study the feasibility of using the SMA for engaging in Solar observations. The overall effort, named *Solar SMA*, aims to provide a synoptic, high-resolution view of the Sun in the submillimeter, leveraging SMA's wide field of view and polarimetric capabilities for exploring dynamic solar phenomena.

Once completed, *Solar SMA* will be capable of continuous solar observing programs, such as active region tracking across the solar disk that would extend for 7-14 days, enabling tracking of energy storage and dissipation over flux emergence time scales of hours to days. Solar SMA will also provide a wealth of data on dynamic events such as solar flares -- allowing for systematic studies of flare sub-THz emission, chromospheric jets and surges, and will be capable of targeting line emission arising from CO and recombination line species, providing important constraints on the temperature structure and evolution of prominences and filaments, coronal rain, coronal mass ejections, and quiet-Sun regions as well as the structure and dynamic. And its near co-location with major solar facilities such as the Daniel K. Inouye Solar Telescope (DKIST) promises to provide an enhanced, panchromatic view of the Sun and its dynamics.

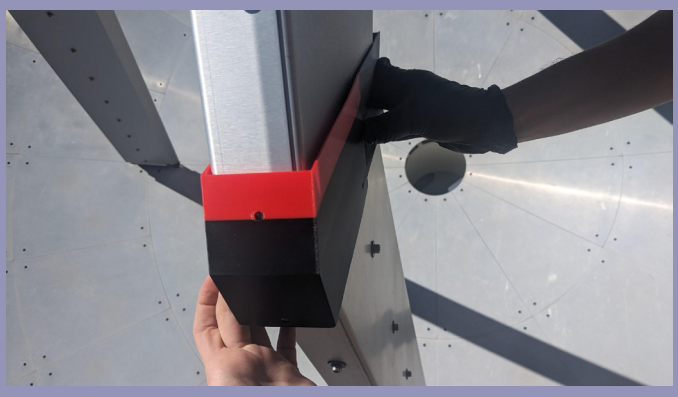

Figure 1: On the summit of Maunakea, CE engineer Abigail Unger performs test fittings of 3D-printed models of the new shielding components. These test fits were successful in verifying dimensional requirements, and came at the conclusion of a multi-year engineering study centered on readying the SMA for solar observing.

The current stage of the study, funded by an internal grant from CfA, has focused on the antenna retrofit work required to sufficiently protect the antennas from the effects of focused sunlight. The SMA has historically had a 25° solar avoidance zone, which was put into place to prevent damage to the secondary support (quadrupod) structure and the electronics contained within. The initial design and engineering effort — completed in September 2023 — aims to remove this restriction with improved radiation shielding and electronics hardening. This included the successful test fitting of prototype, 3D-printed shields on an antenna at the summit of Maunakea. The effort was subsequently funded to conduct a full retrofit of a single antenna, which will enable a telescope operating in single-dish mode for first astronomical SMA measurements of the Sun anticipated in summer/fall 2024.

The Solar SMA team is now working to secure additional funding, with the goal of bringing these new capabilities online in time for the upcoming Solar Maximum, leverage both the current and upcoming capabilities of the wideband SMA (wSMA) upgrade to conduct polarimetric and multi-band observations of the Sun.

[1]Center for Astrophysics | Harvard and Smithsonian

NEW wSMA CRYOSTATS WITH ENHANCED COOLING POWER DELIVERED

Ed Tong[1], on behalf of the wSMA Team

After more than a year of engineering development, the first pair of production wSMA cryostats were delivered to the SMA in December by the vendor High Precision Devices (now part of the company FormFactor). These new wSMA cryostats are equipped with a more powerful cold head than the prototypes, a Cryomech PT-410. As a result, the new cryostats can reach a base temperature of around 3.5 K. Fig. 1 shows the temperature measured at one of the receiver cartridges crossing below 5 K after less than 17 hours of cooldown time. In comparison the prototype cryostat, fitted with the PT-407 cold head, reached a base temperature of 4.2 K after 32 hours of cooldown. The faster cooling rate of the new cryostats comes with only a small increase of power consumption, remaining within the chiller capacity available within the SMA antennas. Moreover, the shorter cooldown time will be a big operational advantage for the SMA.

The enhanced cooling power of the wSMA cryostat will also open up opportunities for future instrumentation development. The receiver cartridges will be able to support a higher heat load, and this can support additional IF amplifiers for greater bandwidth in a single observing band or dual-band operation in a single cartridge. One of the new production cryostats has been set up in the Receiver Lab for preliminary testing (Fig. 2). Integration with wideband wSMA receiver hardware will take place in Cambridge in the next few months. The plan is to deploy one of these new cryostats in the SMA later this year.

At the same time, a prototype wSMA cryostat has been successfully installed in antenna 7 of the SMA (Fig. 3). Test and integration of this cryostat is now in progress

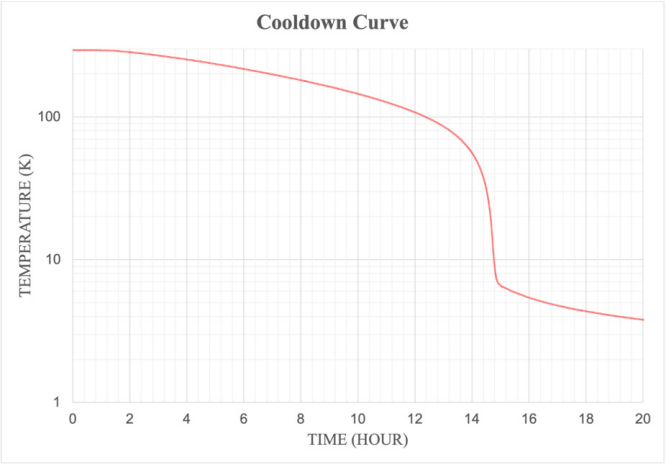

Figure 1: Temperature of a receiver cartridge measured during cooldown of the new wSMA cryostat. A base temperature of 3.5 K was reached 20 hours after the compressor was turned on. At the 18 hour mark, the temperature fell below 4.2 K, the normal maximum operating temperature for SIS mixers.

[1]Center for Astrophysics | Harvard and Smithsonian

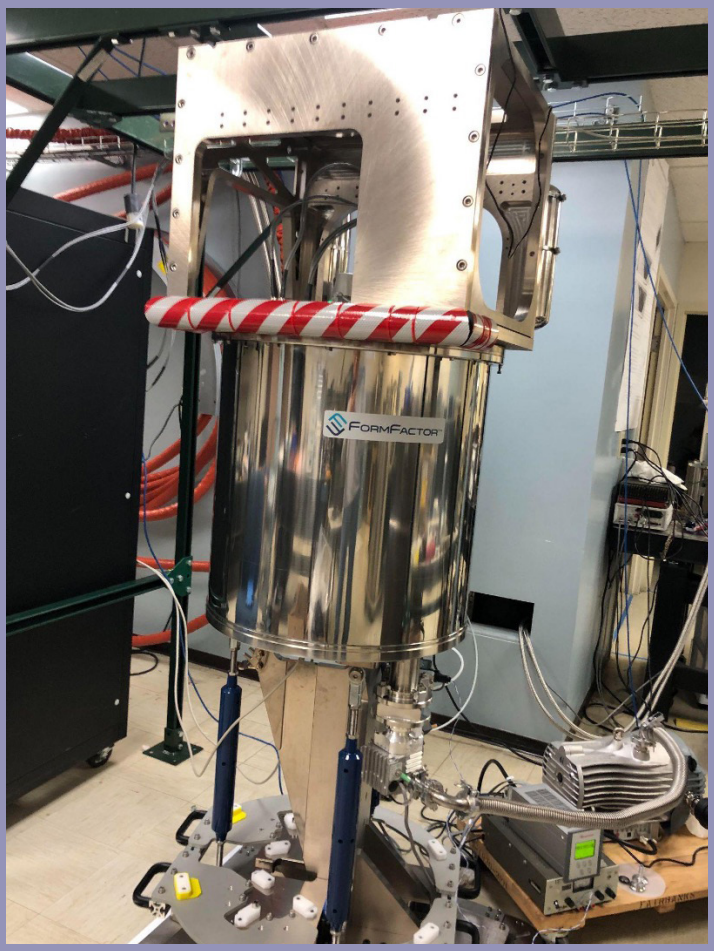

Figure 2: New wSMA cryostat set up in the Receiver Lab in Cambridge for testing.

Figure 3: wSMA Prototype cryostat installed in antenna 7 in the SMA Hangar, Jan 12, 2024.

CALL FOR STANDARD OBSERVING PROPOSALS – 2024A SEMESTER

The next Call for Standard Observing Proposals for observations with the Submillimeter Array (SMA) is for the 2024A semester with observing period nominally **16 May 2024 – 15 Nov 2024** (subject to adjustment as needed).

The deadline for proposals for the 2024A semester will be:
6 March 2024 9PM GMT = 11AM Hawaii, 4PM Cambridge, 5AM 7 March Taipei

The SMA proposal system will open for users to begin crafting their submissions on or near **February 1** at the SMA Observer Center (SMAOC) at **http://sma1.sma.hawaii.edu/call.html** and will include full details on time available, and the proposal submission process.

Details on the SMA capabilities and status can be found at **http://sma1.sma.hawaii.edu/status.html;** proposal creation and submission is also done through the SMAOC at **http://sma1.sma.hawaii.edu/proposing.html.** We are happy to answer any questions and provide assistance in proposal submission; simply email **sma-propose@cfa.harvard.edu** with any inquiries.

Sincerely,

Mark Gurwell, SAO Chair, SMA TAC; Ya-Wen Tang, ASIAA Chair, SMA TAC

PROPOSAL STATISTICS FOR 2023B

The three SMA partner institutions received a total of 66 proposals (53 SAO, 11 ASIAA, 1 UH) and 1 ASIAA Key Project proposal, requesting observing time in the 2023B semester. Since the call, SAO has approved 1 DDT proposal. The 67 proposals were divided among science categories as follows:

CATEGORY	PROPOSALS
local galaxies, starbursts, AGN	16
high mass (OB) star formation, cores	13
protoplanetary, transition, debris disks	11
low/intermediate mass star formation, cores	6
submm/hi-z galaxies	5
galactic center	4
other	4
evolved stars, AGB, PPN	3
solar system	3
GRB, SN, high energy	3

Note that this number of submissions is relatively large, despite PIs knowing that two SAO Large Scale projects were already accepted, and could require up to 30-50% of the available time, suggesting that interest in the SMA is strong and growing as we move out of the pandemic and the SMA capabilities further develop.

2023B TRACK ALLOCATIONS BY WEATHER REQUIREMENT AND CONFIGURATION:

To best accomodate the highest ranked programs from each of the partners, including Large Scale (SAO) and Key Project (ASIAA) programs it was determined that the configuration schedule will be:

COMPACT >> EXTENDED >> SUBCOMPACT >> EXTENDED >> VERY EXTENDED >> COMPACT

Tracks were allocated in the following manner (Std+DDT):

PWV[1]	SAO	ASIAA	UH
< 4.0mm	19A + 45B	18B	5A + 1B
< 2.5mm	20A + 38B	2B	0
< 1.0mm	0	6B	0
Total	**39A + 83B**	**20B**	**5A + 1B**

AO Large Scale and ASIAA Key Projects allocated approximately 30 <4.0mm and 26 <2.5mm tracks[2]

Configuration	SAO	ASIAA	UH
Subcompact	11A + 17B	0	0
Compact	6A + 12B	2B	5A + 1B
Extended	15A + 23B	9B	0
Very Extended	2A + 6B	0	0
Any	5A + 25B	9B	0
Total	**39A + 83B**	**20B**	**5A + 1B**

(1) Precipitable water vapor required for the observations.

(2) One Large Scale program is a time domain project with variable triggering rates based upon random source activity, thus allocations per semester are somewhat uncertain and could potentially exceed the above expectations.

TOP-RANKED 2023B SEMESTER PROPOSALS

The following is the listing of all SAO, ASIAA, and UH proposals with at least one A-rank track allocation along with accepted large scale projects.

EVOLVED STARS, AGB, PPN

2023B-S004 Joel Kastner (RIT)
Mapping the Complex Molecular Envelope of the (Iconic) Ring Nebula, NGC 6720"

GALACTIC CENTER

2023B-S017 Howard Smith (CfA)
SMA Continued Participation in Simultaneous Monitoring, with JWST, of Flaring from the Galactic Center's Supermassive Black Hole
2023B-S052 Garrett "Karto" Keating (CfA)
Polarimetric VLBI for the 2024 Event Horizon Telescope Campaign

GRB, SN, HIGH ENERGY

2022B-S046 Edo Berger (CfA)
POETS: Pursuit of Extragalactic Transients with the SMA [SAO Large Scale]

HIGH MASS (OB) STAR FORMATION, CORES

2023A-A012 Seamus Clarke (ASIAA)
B-fields, gravity and turbulence across multiple scales - How does the relative importance of gravity, turbulence and magnetic fields impact high-mass star and cluster formation? [ASIAA Key Project]
2023B-S002 Qizhou Zhang (CfA)
What drives the starburst in W49A?

LOCAL GALAXIES, STARBURSTS, AGN

2023B-S027 Jakob den Brok (CfA)
Understanding the cause of the drastic decrease of alphaCO in M101
2023B-S030 Steven Willner (CfA)
Disentangling radiating particle properties and jet physics from M87 multi-wavelength variability
2023B-S055 Ivana Beslic (LERMA, ObsP)
Unraveling the Cigar: dense molecular gas across M 82
2023B-S056 Eileen Meyer (UMd-BC)
Probing the nature of the sub-mm continuum in changing-look AGN 1ES 1927+654
2023B-S059 Jakob den Brok (CfA)
DDT: Contrasting the dense gas in AGN vs. starburst environment (AY191 student project)

LOW/INTERMEDIATE MASS STAR FORMATION, CORES

2023B-H001 Suchitra Narayanan (IfA, UH)
Search for small sulfuretted species in 6 chemically rich class 0 protostars in Perseus

OTHER

2023B-S044 Saeqa Vrtilek (CfA)
SMA observations of polarization during a Microquasar outburst.
2023B-S046 Michael McCollough (CfA)
SMA Observations during XRISM and IXPE Observations of Cygnus X-3

PROTOPLANETARY, TRANSITION, DEBRIS DISKS

2022B-S047 Karin Oberg (CfA)
SMA-SPEC: the SMA Survey of Protoplanetary disks to Explore their Chemistry [SAO Large Scale]
2023B-S003 David Wilner (CfA)
A 1.3mm Survey of a New Sample of Herbig Be stars (continued)
2023B-S034 Richard Teague (MIT
A 3D Exploration of an Edge-On Self-Gravitating Disk (VEX Baselines)

SOLAR SYSTEM

2023B-S050 Nathan Roth (NASA GSFC)
Coordinated SMA/ALMA Studies of 12P/Pons-Brooks

SUBMM/HI-Z GALAXIES

2023B-S001 David Clements (ICL)
The Brightest Herschel Galaxies: Lensed or Something Else?
2023B-S051 Garrett "Karto" Keating (CfA)
A Monster, Lurking in the Dark

STANDARD, DDT, AND LARGE SCALE PROJECTS OBSERVED DURING 2023A

SMA Semester 2023A encompassed the period May 24, 2022 through Nov 13, 2023; listed below are all projects that were at least partially completed during the semester.

EVOLVED STARS, AGB, PPN

2023A-S010 Paul Barrett (GWU)
Submillimeter Observations of the Magnetic Propellers in AE Aqr and AR Sco
2023A-S023 Nimesh Patel (CfA)
Chemical Evolution from AGB to PN: A Spectral-line Survey of the Egg Nebula

GALACTIC CENTER

2023A-S050 Farhad Zadeh (Northwestern)
DDT: Simultaneous SMA and JWST Monitoring of Sgr A on August 25, 2023*

GRB, SN, HIGH ENERGY

2022B-S009 Tianyu Tu (Nanjing U.)
Shock and cosmic ray chemistry in molecular clouds interacting with supernova remnant W28
2022B-S046 Edo Berger (CfA)
POETS: Pursuit of Extragalactic Transients with the SMA [SAO Large Scale]

HIGH MASS (OB) STAR FORMATION, CORES

2023A-A003 Han-Tsung Lee (ASIAA)
SDC13.198-0.135 - the infrared dark cloud with spiral magnetic field
2023A-A006 Seamus Clarke (ASIAA)
Linking the fragmentation of clumps to the relative importance of gravity, turbulence and magnetic fields on multiple scales.
2023A-H002 Adwin Boogert (IfA, UH)
Disks in the Binary Massive YSO W3 IRS5
2023A-S009 Qizhou Zhang (CfA)
What drives the starburst in W49A?
2023A-S011 Junhao Liu (EAO)
A dust polarization survey of massive dense cores in Cygnus-X
2023A-S021 Fengwei Xu (Peking U.)
Fragmentation and Mass Segregation Inside the Gas Infalling Massive Clumps by SMA
2023A-S042 Keping Qiu (Nanjing U.)
Surveys of Clumps, Cores, and Condensations in Cygnus X.

LOCAL GALAXIES, STARBURSTS, AGN

2023A-S024 Ioannis Myserlis (IRAM)
SMAPOL: SMA Monitoring of AGNs with POLarization

2023A-S025 Eric Koch (CfA)
Measuring the dust and B-field structure in M33's massive GMCs

2023A-S026 Jean Turner (UCLA)
CO(3-2) n the Dwarf Galaxy NGC 1569

2023A-S028 Jakob den Brok (CfA)
Molecular gas and star formation across the giant and distorted galaxy NGC 1961

2023A-S032 Steven Willner (CfA)
Disentangling radiating particle properties and jet physics from M87 multi-wavelength variability

2023A-S038 Kirsten Hall (CfA)
Direct, observational evidence of AGN feedback on host galaxies' molecular gas

2023A-S046 Eileen Meyer (UMd-BC)
DDT: Millimeter Observations of a Possible Nascent Radio Jet in 1ES 1927+654

LOW/INTERMEDIATE MASS STAR FORMATION, CORES

2023A-A001 Chin-Fei Lee (ASIAA)
Confirming the existence of a proto-brown dwarf candidate in rho Ophiuchus

2023A-A002 Hsi-Wei Yen (ASIAA)
SMA survey of the beginning of star formation and fragmentation in dense cores

OTHER

2022B-S049 Joshua Lovell (CfA)
DDT: What The Flare? Measuring the first-ever T-Tauri Star millimeter flare frequency distribution

2023A-S027 Saeqa Vrtilek (CfA)
Jet Emisson in Microquasars

2023A-S041 Attila Kovacs (CfA)
Resolved SZ imaging of galaxy cluster cores with the SMA

2023A-S043 Michael McCollough (CfA)
DDT: GRS 1915+105 observations coordinated with JWST

PROTOPLANETARY, TRANSITION, DEBRIS DISKS

2022B-S047 Karin Oberg (CfA)
SMA-SPEC: the SMA Survey of Protoplanetary disks to Explore their Chemistry [SAO Large Scale]

2023A-A009 Chia-Ying Chung (ASIAA)
A statistical study to constrain grain growth efficiency in protoplanetary disks

2023A-S003 Sean Andrews (CfA)
Mitigating "Survivor Bias" in Constraints on Disk Evolution

2023A-S017 David Wilner (CfA)
A 1.3mm Survey of a New Sample of Herbig Be stars

2023A-S019 Charles Law (CfA)
HNC as a Novel Tracer of Protoplanetary Disk Properties

2023A-S052 Joshua Lovell (CfA)
DDT: The first arcsecond millimeter view of the giant edge-on disk: Dracula's Chivito

SOLAR SYSTEM

2023A-A008 Wei-Ling Tseng (NTNU)
Monitoring Io's dynamical volcanic eruptions and their contributions to Jupiter's magnetosphere (continuation)

2023A-S006 Alex Akins (JPL)
Dynamics in Uranus' Troposphere

SUBMM/HI-Z GALAXIES

2022B-S039 Luwenjia Zhou (Nanjing U.)
A systematic survey on the dust/gas emission of cluster galaxies in the early Universe

2023A-H001 Lennox Cowie (IfA, UH)
JWST *and* SCUBA-2: A Powerful *Combination for Studying Submm Galaxies*

2023A-S022 Giovanni G. Fazio (CfA)
Understanding the Evolution of Obscured Activity Out to z>3 -- A SMA Survey of Submillimeter Sources in the JWST Time Domain Field

2023A-S049 Kirsten Hall (CfA)
DDT: Higher resolution continuum fluxes of ACT-selected DSFGs: A case for multiple components

RECENT PUBLICATIONS

TITLE: Multiband cross-correlated radio variability of the blazar 3C 279
AUTHOR: Mohana A, K., Gupta, A. C., Marscher, A. P., Sotnikova, Y. V., Jorstad, S. G., Wiita, P. J., Cui, L., Aller, M. F., Aller, H. D., Kovalev, Y. A., Kovalev, Y. Y., Liu, X., Mufakharov, T. V., Popkov, A. V., Mingaliev, M. G., Erkenov, A. K., Nizhelsky, N. A., Tsybulev, P. G., Zhao, W., Weaver, Z. R., Morozova, D. A.
PUBLICATION: *Monthly Notices of the Royal Astronomical Society, 527, 6970-6980*
PUBLICATION DATE: 01/2024
ABSTRACT: *https://ui.adsabs.harvard.edu/abs/2024MNRAS.527.6970M*
DOI: 10.1093/mnras/stad3583

TITLE: Interstellar complex organic molecules towards outflows from the G351.16+0.70 (NGC 6334 V) massive protostellar system
AUTHOR: Rojas-García, O. S., Gómez-Ruiz, A. I., Palau, A., Orozco-Aguilera, M. T., Kurtz, S. E., Chavez Dagostino, M.
PUBLICATION: *Monthly Notices of the Royal Astronomical Society, 527, 2110-2127*
PUBLICATION DATE: 01/2024
ABSTRACT: *https://ui.adsabs.harvard.edu/abs/2024MNRAS.527.2110R*
DOI: 10.1093/mnras/stad3161

TITLE: A near magnetic-to-kinetic energy equipartition flare from the relativistic jet in AO 0235 + 164 during 2013-2019
AUTHOR: Cheong, W. Y., Lee, S.-S., Kim, S.-H., Kang, S., Kim, J. Y., Rani, B., Readhead, A. C. S., Kiehlmann, S., Lähteenmäki, A., Tornikoski, M., Tammi, J., Ramakrishnan, V., Agudo, I., Fuentes, A., Traianou, E., Escudero, J., Thum, C., Myserlis, I., Casadio, C., Gurwell, M.
PUBLICATION: *Monthly Notices of the Royal Astronomical Society, 527, 882-894*
PUBLICATION DATE: 01/2024
ABSTRACT: *https://ui.adsabs.harvard.edu/abs/2024MNRAS.527..882C*
DOI: 10.1093/mnras/stad3250

TITLE: On the Origin of the X-ray Emission in Heavily Obscured Compact Radio Sources
AUTHOR: Król, D. Ł., Sobolewska, M., Stawarz, Ł., Siemiginowska, A., Migliori, G., Principe, G., Gurwell, M. A.
PUBLICATION: *arXiv e-prints, arXiv:2312.13418*
PUBLICATION DATE: 12/2023
ABSTRACT: *https://ui.adsabs.harvard.edu/abs/2023arXiv231213418K*
DOI: 10.48550/arXiv.2312.13418

TITLE: First characterization of the emission behavior of Mrk421 from radio to VHE gamma rays with simultaneous X-ray polarization measurements
AUTHOR: Abe, S., Abhir, J., Acciari, V. A., Agudo, I., Aniello, T., Ansoldi, S., Antonelli, L. A., Arbet Engels, A., Arcaro, C., Artero, M., Asano, K., Babić, A., Baquero, A., Barres de Almeida, U., Barrio, J. A., Batković, I., Baxter, J., Becerra González, J., Bednarek, W., Bernardini, E., Bernete, J., Berti, A., Besenrieder, J., Bigongiari, C., Biland, A., Blanch, O., Bonnoli, G., Bošnjak, Ž., Burelli, I., Busetto, G., Campoy-Ordaz, A., Carosi, A., Carosi, R., Carretero-Castrillo, M., Castro-Tirado, A. J., Ceribella, G., Chai, Y., Cifuentes, A., Cikota, S., Colombo, E., Contreras, J. L., Cortina, J., Covino, S., D'Ammando, F.,

D'Amico, G., D'Elia, V., Da Vela, P., Dazzi, F., De Angelis, A., De Lotto, B., de Menezes, R., Del Popolo, A., Delgado, J., Delgado Mendez, C., Di Pierro, F., Di Venere, L., Dominis Prester, D., Donini, A., Dorner, D., Doro, M., Elsaesser, D., Emery, G., Escudero, J., Fariña, L., Fattorini, A., Foffano, L., Font, L., Fröse, S., Fukami, S., Fukazawa, Y., García López, R. J., Garczarczyk, M., Gasparyan, S., Gaug, M., Giesbrecht Paiva, J. G., Giglietto, N., Giordano, F., Gliwny, P., Godinović, N., Gradetzke, T., Grau, R., Green, D., Green, J. G., Günther, P., Hadasch, D., Hahn, A., Hassan, T., Heckmann, L., Herrera, J., Hrupec, D., Hütten, M., Imazawa, R., Inada, T., Ishio, K., Jiménez Martínez, I., Jormanainen, J., Kerszberg, D., Kluge, G. W., Kobayashi, Y., Kouch, P. M., Kubo, H., Kushida, J., Láinez Lezáun, M., Lamastra, A., Leone, F., Lindfors, E., Linhoff, L., Lombardi, S., Longo, F., López-Coto, R., López-Moya, M., López-Oramas, A., Loporchio, S., Lorini, A., Machado de Oliveira Fraga, B., Majumdar, P., Makariev, M., Maneva, G., Mang, N., Manganaro, M., Mangano, S., Mannheim, K., Mariotti, M., Martínez, M., Martínez-Chicharro, M., Mas-Aguilar, A., Mazin, D., Menchiari, S., Mender, S., Miceli, D., Miener, T., Miranda, J. M., Mirzoyan, R., Molero González, M., Molina, E., Mondal, H. A., Moralejo, A., Morcuende, D., Nakamori, T., Nanci, C., Nava, L., Neustroev, V., Nickel, L., Nievas Rosillo, M., Nigro, C., Nikolić, L., Nilsson, K., Nishijima, K., Njoh Ekoume, T., Noda, K., Nozaki, S., Ohtani, Y., Okumura, A., Otero-Santos, J., Paiano, S., Palatiello, M., Paneque, D., Paoletti, R., Paredes, J. M., Pavlović, D., Peresano, M., Persic, M., Pihet, M., Pirola, G., Podobnik, F., Prada Moroni, P. G., Prandini, E., Principe, G., Priyadarshi, C., Rhode, W., Ribó, M., Rico, J., Righi, C., Sahakyan, N., Saito, T., Satalecka, K., Saturni, F. G., Schleicher, B., Schmidt, K., Schmuckermaier, F., Schubert, J. L., Schweizer, T., Sciaccaluga, A., Sitarek, J., Sliusar, V., Sobczynska, D., Stamerra, A., Strišković, J., Strom, D., Strzys, M., Suda, Y., Suutarinen, S., Tajima, H., Takahashi, M., Takeishi, R., Tavecchio, F., Temnikov, P., Terauchi, K., Terzić, T., Teshima, M., Tosti, L., Truzzi, S., Tutone, A., Ubach, S., van Scherpenberg, J., Vazquez Acosta, M., Ventura, S., Viale, I., Vigorito, C. F., Vitale, V., Vovk, I., Walter, R., Will, M., Wunderlich, C., Yamamoto, T., Liodakis, I., Jorstad, S. G., Gesu, L. D., Donnarumma, I., Kim, D. E., Marscher, A. P., Middei, R., Perri, M., Puccetti, S., Verrecchia, F., Leto, C., De La Calle Pérez, I., Jiménez-Bailón, E., Blinov, D., Bourbah, I. G., Kiehlmann, S., Kontopodis, E., Mandarakas, N., Skalidis, R., Vervelaki, A., Aceituno, F. J., Agís-González, B., Sota, A., Sasada, M., Fukazawa, Y., Kawabata, K. S., Uemura, M., Mizuno, T., Akitaya, H., Casadio, C., Myserlis, I., Sievers, A., Lähteenmäki, A., Syrjärinne, I., Tornikoski, M., Salomé, Q., Gurwell, M., Keating, G. K., Rao, R.

PUBLICATION: *arXiv e-prints, arXiv:2312.10732*
PUBLICATION DATE: 12/2023
ABSTRACT: *https://ui.adsabs.harvard.edu/abs/2023arXiv231210732A*
DOI: 10.48550/arXiv.2312.10732

TITLE: CMZoom IV. Incipient High-Mass Star Formation Throughout the Central Molecular Zone
AUTHOR: Hatchfield, H. P., Battersby, C., Barnes, A. T., Butterfield, N., Ginsburg, A., Henshaw, J. D., Longmore, S. N., Lu, X., Svoboda, B., Walker, D., Callanan, D., Mills, E. A. C., Ho, L. C., Kauffmann, J., Kruijssen, J. M. D., Ott, J., Pillai, T., Zhang, Q.
PUBLICATION: *arXiv e-prints, arXiv:2312.09284*
PUBLICATION DATE: 12/2023
ABSTRACT: *https://ui.adsabs.harvard.edu/abs/2023arXiv231209284H*
DOI: 10.48550/arXiv.2312.09284

TITLE: Surveys of clumps, cores, and condensations in Cygnus-X: SMA observations of SiO (5$-$4)
AUTHOR: Yang, K., Qiu, K., Pan, X.
PUBLICATION: *arXiv e-prints, arXiv:2312.04880*
PUBLICATION DATE: 12/2023
ABSTRACT: *https://ui.adsabs.harvard.edu/abs/2023arXiv231204880Y*
DOI: 10.48550/arXiv.2312.04880

TITLE: X-ray detection of the most extreme star-forming galaxies at the cosmic noon via strong lensing
AUTHOR: Wang, Q. D., Diaz, C. G., Kamieneski, P. S., Harrington, K. C., Yun, M. S., Foo, N., Frye, B. L., Jimenez-Andrade, E. F., Liu, D., Lowenthal, J. D., Pampliega, B. A., Pascale, M., Vishwas, A., Gurwell, M. A.
PUBLICATION: *Monthly Notices of the Royal Astronomical Society,*
PUBLICATION DATE: 12/2023
ABSTRACT: *https://ui.adsabs.harvard.edu/abs/2023MNRAS.tmp.3662W*
DOI: 10.1093/mnras/stad3827

TITLE: X-Ray Polarization of the BL Lacertae Type Blazar 1ES 0229+200

AUTHOR: Ehlert, S. R., Liodakis, I., Middei, R., Marscher, A. P., Tavecchio, F., Agudo, I., Kouch, P. M., Lindfors, E., Nilsson, K., Myserlis, I., Gurwell, M., Rao, R., Aceituno, F. J., Bonnoli, G., Casanova, V., Agís-González, B., Escudero, J., Husillos, C., Otero Santos, J., Sota, A., Angelakis, E., Kraus, A., Keating, G. K., Antonelli, L. A., Bachetti, M., Baldini, L., Baumgartner, W. H., Bellazzini, R., Bianchi, S., Bongiorno, S. D., Bonino, R., Brez, A., Bucciantini, N., Capitanio, F., Castellano, S., Cavazzuti, E., Chen, C.-T., Ciprini, S., Costa, E., De Rosa, A., Del Monte, E., Di Gesu, L., Di Lalla, N., Di Marco, A., Donnarumma, I., Doroshenko, V., Dovčiak, M., Enoto, T., Evangelista, Y., Fabiani, S., Ferrazzoli, R., Garcia, J. A., Gunji, S., Hayashida, K., Heyl, J., Iwakiri, W., Jorstad, S. G., Kaaret, P., Karas, V., Kislat, F., Kitaguchi, T., Kolodziejczak, J. J., Krawczynski, H., La Monaca, F., Latronico, L., Maldera, S., Manfreda, A., Marin, F., Marinucci, A., Marshall, H. L., Massaro, F., Matt, G., Mitsuishi, I., Mizuno, T., Muleri, F., Negro, M., Ng, C.-Y., O'Dell, S. L., Omodei, N., Oppedisano, C., Papitto, A., Pavlov, G. G., Peirson, A. L., Perri, M., Pesce-Rollins, M., Petrucci, P.-O., Pilia, M., Possenti, A., Poutanen, J., Puccetti, S., Ramsey, B. D., Rankin, J., Ratheesh, A., Roberts, O. J., Romani, R. W., Sgró, C., Slane, P., Soffitta, P., Spandre, G., Swartz, D. A., Tamagawa, T., Taverna, R., Tawara, Y., Tennant, A. F., Thomas, N. E., Tombesi, F., Trois, A., Tsygankov, S. S., Turolla, R., Vink, J., Weisskopf, M. C., Wu, K., Xie, F., Zane, S.

PUBLICATION: *The Astrophysical Journal, 959, 61*

PUBLICATION DATE: 12/2023

ABSTRACT: *https://ui.adsabs.harvard.edu/abs/2023ApJ...959...61E*

DOI: 10.3847/1538-4357/ad05c4

TITLE: RZ Piscium Hosts a Compact and Highly Perturbed Debris Disk

AUTHOR: Su, K. Y. L., Kennedy, G. M., Rieke, G. H., Hughes, A. M., Lin, Y.-C., Kittling, J., Jackson, A. P., Anche, R. M., Liu, H. B.

PUBLICATION: *The Astrophysical Journal, 959, 43*

PUBLICATION DATE: 12/2023

ABSTRACT: *https://ui.adsabs.harvard.edu/abs/2023ApJ...959...43S*

DOI: 10.3847/1538-4357/ad04d9

TITLE: Density distributions, magnetic field structures and fragmentation in high-mass star formation

AUTHOR: Beuther, H., Gieser, C., Soler, J. D., Zhang, Q., Rao, R., Semenov, D., Henning, T., Pudritz, R., Peters, T., Klaassen, P., Beltran, M. T., Palau, A., Moeller, T., Johnston, K. G., Zinnecker, H., Urquhart, J., Kuiper, R., Ahmadi, A., Sanchez-Monge, A., Feng, S., Leurini, S., Ragan, S. E.

PUBLICATION: *arXiv e-prints, arXiv:2311.11874*

PUBLICATION DATE: 11/2023

ABSTRACT: *https://ui.adsabs.harvard.edu/abs/2023arXiv231111874B*

DOI: 10.48550/arXiv.2311.11874

TITLE: Chasing the Break: Tracing the full evolution of a black hole X-ray binary jet with multi-wavelength spectral modeling

AUTHOR: Echiburú-Trujillo, C., Tetarenko, A. J., Haggard, D., Russell, T. D., Koljonen, K. I. I., Bahramian, A., Wang, J., Bremer, M., Bright, J., Casella, P., Russell, D. M., Altamirano, D., Baglio, M. C., Belloni, T., Ceccobello, C., Corbel, S., Diaz Trigo, M., Maitra, D., Gabuya, A., Gallo, E., Heinz, S., Homan, J., Kara, E., Körding, E., Lewis, F., Lucchini, M., Markoff, S., Migliari, S., Miller-Jones, J. C. A., Rodriguez, J., Saikia, P., Sarazin, C. L., Shahbaz, T., Sivakoff, G., Soria, R., Testa, V., Tetarenko, B. E., Tudose, V.

PUBLICATION: *arXiv e-prints, arXiv:2311.11523*

PUBLICATION DATE: 11/2023

ABSTRACT: *https://ui.adsabs.harvard.edu/abs/2023arXiv231111523E*

DOI: 10.48550/arXiv.2311.11523

TITLE: Minutes-duration optical flares with supernova luminosities

AUTHOR: Ho, A. Y. Q., Perley, D. A., Chen, P., Schulze, S., Dhillon, V., Kumar, H., Suresh, A., Swain, V., Bremer, M., Smartt, S. J., Anderson, J. P., Anupama, G. C., Awiphan, S., Barway, S., Bellm, E. C., Ben-Ami, S., Bhalerao, V., de Boer, T., Brink, T. G., Burruss, R., Chandra, P., Chen, T.-W., Chen, W.-P., Cooke, J., Coughlin, M. W., Das, K. K., Drake, A. J., Filippenko, A. V., Freeburn, J., Fremling, C., Fulton, M. D., Gal-Yam, A., Galbany, L., Gao, H., Graham, M. J., Gromadzki, M., Gutiérrez, C. P., Hinds, K.-R., Inserra, C., A J, N., Karambelkar, V., Kasliwal, M. M., Kulkarni, S., Müller-Bravo, T. E., Magnier, E. A., Mahabal, A. A., Moore, T., Ngeow, C.-C., Nicholl, M., Ofek, E. O., Omand, C. M. B., Onori, F., Pan, Y.-C., Pessi, P. J., Petitpas, G., Polishook, D., Poshyachinda, S., Pursiainen, M., Riddle, R., Rodriguez, A. C., Rusholme, B., Segre, E., Sharma, Y., Smith, K. W., Sollerman, J., Srivastav, S., Strotjohann, N. L., Suhr, M., Svinkin, D., Wang, Y., Wiseman, P., Wold, A., Yang, S., Yang, Y., Yao, Y., Young, D. R., Zheng, W.

PUBLICATION: *Nature, 623, 927-931*

PUBLICATION DATE: 11/2023

ABSTRACT: *https://ui.adsabs.harvard.edu/abs/2023Natur.623..927H*

DOI: 10.1038/s41586-023-06673-6

TITLE: Tracing dense gas in six resolved GMCs of the Andromeda Galaxy

AUTHOR: Forbrich, J., Lada, C. J., Pety, J., Petitpas, G.

PUBLICATION: *Monthly Notices of the Royal Astronomical Society, 525, 5565-5574*

PUBLICATION DATE: 11/2023

ABSTRACT: *https://ui.adsabs.harvard.edu/abs/2023MNRAS.525.5565F*

DOI: 10.1093/mnras/stad2600

TITLE: Hidden giants in JWST's PEARLS: An ultra-massive z=4.26 sub-millimeter galaxy that is invisible to HST

AUTHOR: Smail, I., Dudzeviciute, U., Gurwell, M., Fazio, G. G., Willner, S. P., Swinbank, A. M., Arumugam, V., Summers, J., Cohen, S. H., Jansen, R. A., Windhorst, R. A., Meena, A., Zitrin, A., Keel, W. C., Coe, D., Conselice, C. J., D'Silva, J. C. J., Driver, S. P., Frye, B., Grogin, N. A., Koekemoer, A. M., Marshall, M. A., Nonino, M., Pirzkal, N., Robotham, A., Rutkowski, M. J., Ryan, R. E., Tompkins, S., Willmer, C. N. A., Yan, H., Broadhurst, T. J., Cheng, C., Diego, J. M., Kamieneski, P., Yun, M.

PUBLICATION: *The Astrophysical Journal, 958, 36*

PUBLICATION DATE: 11/2023

ABSTRACT: *https://ui.adsabs.harvard.edu/abs/2023ApJ...958...36S*

DOI: 10.3847/1538-4357/acf931

TITLE: Polarimetric Geometric Modeling for mm-VLBI Observations of Black Holes

AUTHOR: Roelofs, F., Johnson, M. D., Chael, A., Janssen, M., Wielgus, M., Broderick, A. E., Akiyama, K., Alberdi, A., Alef, W., Algaba, J. C., Anantua, R., Asada, K., Azulay, R., Bach, U., Baczko, A.-K., Ball, D., Baloković, M., Barrett, J., Bauböck, M., Benson, B. A., Bintley, D., Blackburn, L., Blundell, R., Bouman, K. L., Bower, G. C., Boyce, H., Bremer, M., Brinkerink, C. D., Brissenden, R., Britzen, S., Broguiere, D., Bronzwaer, T., Bustamante, S., Byun, D.-Y., Carlstrom, J. E., Ceccobello, C., Chan, C.-. kwan ., Chang, D. O., Chatterjee, K., Chatterjee, S., Chen, M.-T., Chen, Y., Cheng, X., Cho, I., Christian, P., Conroy, N. S., Conway, J. E., Cordes, J. M., Crawford, T. M., Crew, G. B., Cruz-Osorio, A., Cui, Y., Dahale, R., Davelaar, J., De Laurentis, M., Deane, R., Dempsey, J., Desvignes, G., Dexter, J., Dhruv, V., Doeleman, S. S., Dougal, S., Dzib, S. A., Eatough, R. P., Emami, R., Falcke, H., Farah, J., Fish, V. L., Fomalont, E., Ford, H. A., Foschi, M., Fraga-Encinas, R., Freeman, W. T., Friberg, P., Fromm, C. M., Fuentes, A., Galison, P., Gammie, C. F., García, R., Gentaz, O., Georgiev, B., Goddi, C., Gold, R., Gómez-Ruiz, A. I., Gómez, J. L., Gu, M., Gurwell, M., Hada, K., Haggard, D., Haworth, K., Hecht, M. H., Hesper, R., Heumann, D., Ho, L. C., Ho, P., Honma, M., Huang, C.-W. L., Huang, L., Hughes, D. H., Ikeda, S., Impellizzeri, C. M. V., Inoue, M., Issaoun, S., James, D. J., Jannuzi, B. T., Jeter, B., Jiang, W., Jiménez-Rosales, A., Jorstad, S., Joshi, A. V., Jung, T., Karami, M., Karuppusamy, R., Kawashima, T., Keating, G. K., Kettenis, M., Kim, D.-J., Kim, J.-Y., Kim, J., Kim, J., Kino, M., Koay, J. Y., Kocherlakota, P., Kofuji, Y., Koch, P. M., Koyama, S., Kramer, C., Kramer, J. A., Kramer, M., Krichbaum, T. P., Kuo, C.-Y., La Bella, N., Lauer, T. R., Lee, D., Lee, S.-S., Leung, P. K., Levis, A., Li, Z., Lico, R., Lindahl, G., Lindqvist, M., Lisakov, M., Liu, J., Liu, K., Liuzzo, E., Lo, W.-P., Lobanov, A. P., Loinard, L., Lonsdale, C. J., Lowitz, A. E., Lu, R.-S., MacDonald, N. R., Mao, J., Marchili, N., Markoff, S., Marrone, D. P., Marscher, A. P., Martí-Vidal, I., Matsushita, S., Matthews, L. D., Medeiros, L., Menten, K. M., Michalik, D., Mizuno, I., Mizuno, Y., Moran, J. M., Moriyama, K.,

Moscibrodzka, M., Mulaudzi, W., Müller, C., Müller, H., Mus, A., Musoke, G., Myserlis, I., Nadolski, A., Nagai, H., Nagar, N. M., Nakamura, M., Narayanan, G., Natarajan, I., Nathanail, A., Fuentes, S. N., Neilsen, J., Neri, R., Ni, C., Noutsos, A., Nowak, M. A., Oh, J., Okino, H., Olivares, H., Ortiz-León, G. N., Oyama, T., Özel, F., Palumbo, D. C. M., Paraschos, G. F., Park, J., Parsons, H., Patel, N., Pen, U.-L., Pesce, D. W., Piétu, V., Plambeck, R., PopStefanija, A., Porth, O., Pötzl, F. M., Prather, B., Preciado-López, J. A., Psaltis, D., Pu, H.-Y., Ramakrishnan, V., Rao, R., Rawlings, M. G., Raymond, A. W., Rezzolla, L., Ricarte, A., Ripperda, B., Rogers, A., Romero-Cañizales, C., Ros, E., Roshanineshat, A., Rottmann, H., Roy, A. L., Ruiz, I., Ruszczyk, C., Rygl, K. L. J., Sánchez, S., Sánchez-Argüelles, D., Sánchez-Portal, M., Sasada, M., Satapathy, K., Savolainen, T., Schloerb, F. P., Schonfeld, J., Schuster, K.-F., Shao, L., Shen, Z., Small, D., Sohn, B. W., SooHoo, J., Sosapanta Salas, L. D., Souccar, K., Sun, H., Tazaki, F., Tetarenko, A. J., Tiede, P., Tilanus, R. P. J., Titus, M., Torne, P., Toscano, T., Traianou, E., Trent, T., Trippe, S., Turk, M., van Bemmel, I., van Langevelde, H. J., van Rossum, D. R., Vos, J., Wagner, J., Ward-Thompson, D., Wardle, J., Washington, J. E., Weintroub, J., Wharton, R., Wiik, K., Witzel, G., Wondrak, M. F., Wong, G. N., Wu, Q., Yadlapalli, N., Yamaguchi, P., Yfantis, A., Yoon, D., Young, A., Young, K., Younsi, Z., Yu, W., Yuan, F., Yuan, Y.-F., Zensus, J. A., Zhang, S., Zhao, G.-Y., Zhao, S.-S.

PUBLICATION: *The Astrophysical Journal, 957, L21*
PUBLICATION DATE: 11/2023
ABSTRACT: *https://ui.adsabs.harvard.edu/abs/2023ApJ...957L..21R*
DOI: 10.3847/2041-8213/acff6f

TITLE: First M87 Event Horizon Telescope Results. IX. Detection of Near-horizon Circular Polarization
AUTHOR: Event Horizon Telescope Collaboration, Akiyama, K., Alberdi, A., Alef, W., Algaba, J. C., Anantua, R., Asada, K., Azulay, R., Bach, U., Baczko, A.-K., Ball, D., Baloković, M., Barrett, J., Bauböck, M., Benson, B. A., Bintley, D., Blackburn, L., Blundell, R., Bouman, K. L., Bower, G. C., Boyce, H., Bremer, M., Brinkerink, C. D., Brissenden, R., Britzen, S., Broderick, A. E., Broguiere, D., Bronzwaer, T., Bustamante, S., Byun, D.-Y., Carlstrom, J. E., Ceccobello, C., Chael, A., Chan, C.-. kwan ., Chang, D. O., Chatterjee, K., Chatterjee, S., Chen, M.-T., Chen, Y., Cheng, X., Cho, I., Christian, P., Conroy, N. S., Conway, J. E., Cordes, J. M., Crawford, T. M., Crew, G. B., Cruz-Osorio, A., Cui, Y., Dahale, R., Davelaar, J., De Laurentis, M., Deane, R., Dempsey, J., Desvignes, G., Dexter, J., Dhruv, V., Doeleman, S. S., Dougal, S., Dzib, S. A., Eatough, R. P., Emami, R., Falcke, H., Farah, J., Fish, V. L., Fomalont, E., Ford, H. A., Foschi, M., Fraga-Encinas, R., Freeman, W. T., Friberg, P., Fromm, C. M., Fuentes, A., Galison, P., Gammie, C. F., García, R., Gentaz, O., Georgiev, B., Goddi, C., Gold, R., Gómez-Ruiz, A. I., Gómez, J. L., Gu, M., Gurwell, M., Hada, K., Haggard, D., Haworth, K., Hecht, M. H., Hesper, R., Heumann, D., Ho, L. C., Ho, P., Honma, M., Huang, C.-W. L., Huang, L., Hughes, D. H., Ikeda, S., Impellizzeri, C. M. V., Inoue, M., Issaoun, S., James, D. J., Jannuzi, B. T., Janssen, M., Jeter, B., Jiang, W., Jiménez-Rosales, A., Johnson, M. D., Jorstad, S., Joshi, A. V., Jung, T., Karami, M., Karuppusamy, R., Kawashima, T., Keating, G. K., Kettenis, M., Kim, D.-J., Kim, J.-Y., Kim, J., Kim, J., Kino, M., Koay, J. Y., Kocherlakota, P., Kofuji, Y., Koch, P. M., Koyama, S., Kramer, C., Kramer, J. A., Kramer, M., Krichbaum, T. P., Kuo, C.-Y., La Bella, N., Lauer, T. R., Lee, D., Lee, S.-S., Leung, P. K., Levis, A., Li, Z., Lico, R., Lindahl, G., Lindqvist, M., Lisakov, M., Liu, J., Liu, K., Liuzzo, E., Lo, W.-P., Lobanov, A. P., Loinard, L., Lonsdale, C. J., Lowitz, A. E., Lu, R.-S., MacDonald, N. R., Mao, J., Marchili, N., Markoff, S., Marrone, D. P., Marscher, A. P., Martí-Vidal, I., Matsushita, S., Matthews, L. D., Medeiros, L., Menten, K. M., Michalik, D., Mizuno, I., Mizuno, Y., Moran, J. M., Moriyama, K., Moscibrodzka, M., Mulaudzi, W., Müller, C., Müller, H., Mus, A., Musoke, G., Myserlis, I., Nadolski, A., Nagai, H., Nagar, N. M., Nakamura, M., Narayan, R., Narayanan, G., Natarajan, I., Nathanail, A., Fuentes, S. N., Neilsen, J., Neri, R., Ni, C., Noutsos, A., Nowak, M. A., Oh, J., Okino, H., Olivares, H., Ortiz-León, G. N., Oyama, T., Özel, F., Palumbo, D. C. M., Paraschos, G. F., Park, J., Parsons, H., Patel, N., Pen, U.-L., Pesce, D. W., Piétu, V., Plambeck, R., PopStefanija, A., Porth, O., Pötzl, F. M., Prather, B., Preciado-López, J. A., Psaltis, D., Pu, H.-Y., Ramakrishnan, V., Rao, R., Rawlings, M. G., Raymond, A. W., Rezzolla, L., Ricarte, A., Ripperda, B., Roelofs, F., Rogers, A., Romero-Cañizales, C., Ros, E., Roshanineshat, A., Rottmann, H., Roy, A. L., Ruiz, I., Ruszczyk, C., Rygl, K. L. J., Sánchez, S., Sánchez-Argüelles, D., Sánchez-Portal, M., Sasada, M., Satapathy, K., Savolainen, T., Schloerb, F. P., Schonfeld, J., Schuster, K.-F., Shao, L., Shen, Z., Small, D., Sohn, B. W., SooHoo, J., Sosapanta Salas, L. D., Souccar, K., Sun, H., Tazaki, F., Tetarenko, A. J., Tiede, P., Tilanus, R. P. J., Titus, M., Torne, P., Toscano, T., Traianou, E., Trent, T., Trippe, S., Turk, M., van Bemmel, I., van Langevelde, H. J., van Rossum, D. R., Vos, J., Wagner, J., Ward-Thompson, D., Wardle, J., Washington, J. E., Weintroub, J., Wharton, R., Wielgus, M., Wiik, K., Witzel, G., Wondrak, M. F., Wong, G. N., Wu, Q., Yadlapalli, N., Yamaguchi, P., Yfantis, A., Yoon, D., Young, A., Young, K., Younsi, Z., Yu, W., Yuan, F., Yuan, Y.-F., Zensus, J. A., Zhang, S., Zhao, G.-Y., Zhao, S.-S.

PUBLICATION: *The Astrophysical Journal, 957, L20*
PUBLICATION DATE: 11/2023
ABSTRACT: *https://ui.adsabs.harvard.edu/abs/2023ApJ...957L..20E*
DOI: 10.3847/2041-8213/acff70

TITLE: Magnetic Field Properties inside the Jet of Mrk 421: Multiwavelength Polarimetry Including the Imaging X-ray Polarimetry Explorer

AUTHOR: Kim, D. E., Di Gesu, L., Liodakis, I., Marscher, A. P., Jorstad, S. G., Midde, R., Marshall, H. L., Pacciani, L., Agudo, I., Tavecchio, F., Cibrario, N., Tugliani, S., Bonino, R., Negro, M., Puccetti, S., Tombesi, F., Costa, E., Donnarumma, I., Soffitta, P., Mizuno, T., Fukazawa, Y., Kawabata, K. S., Nakaoka, T., Uemura, M., Imazawa, R., Sasada, M., Akitaya, H., Josè Aceituno, F., Bonnoli, G., Casanova, V., Myserlis, I., Sievers, A., Angelakis, E., Kraus, A., Cheong, W. Y., Jeong, H.-W., Kang, S., Kim, S.-H., Lee, S.-S., Agìs-Gonzàlez, B., Sota, A., Escudero, J., Gurwell, M., Keating, G. K., Rao, R., Kouch, P. M., Lindfors, E., Bourbah, I. G., Kiehlmann, S., Kontopodis, E., Mandarakas, N., Romanopoulos, S., Skalidis, R., Vervelaki, A., Savchenko, S. S., Antonelli, L. A., Bachetti, M., Baldini, L., Baumgartner, W. H., Bellazzini, R., Bianchi, S., Bongiorno, S. D., Brez, A., Bucciantini, N., Capitanio, F., Castellano, S., Cavazzuti, E., Chen, C.-T., Ciprini, S., De Rosa, A., Del Monte, E., Di Lalla, N., Di Marco, A., Doroshenko, V., Dovčiak, M., Ehlert, S. R., Enoto, T., Evangelista, Y., Fabiani, S., Ferrazzoli, R., Garcia, J. A., Gunji, S., Hayashida, K., Heyl, J., Iwakiri, W., Kaaret, P., Karas, V., Kislat, F., Kitaguchi, T., Kolodziejczak, J. J., Krawczynski, H., La Monaca, F., Latronico, L., Maldera, S., Manfreda, A., Marin, F., Marinucci, A., Massaro, F., Matt, G., Mitsuishi, I., Muleri, F., Ng, C.-Y., O'Dell, S. L., Omodei, N., Oppedisano, C., Papitto, A., Pavlov, G. G., Peirson, A. L., Perri, M., Pesce-Rollins, M., Petrucci, P.-O., Pilia, M., Possenti, A., Poutanen, J., Ramsey, B. D., Rankin, J., Ratheesh, A., Roberts, O., Romani, R. W., Sgrò, C., Slane, P., Spandre, G., Swartz, D., Tamagawa, T., Taverna, R., Tawara, Y., Tennant, A. F., Thomas, N. E., Trois, A., Tsygankov, S. S., Turolla, R., Vink, J., Weisskopf, M. C., Wu, K., Xie, F., Zane, S.

PUBLICATION: *arXiv e-prints, arXiv:2310.06097*

PUBLICATION DATE: 10/2023

ABSTRACT: *https://ui.adsabs.harvard.edu/abs/2023arXiv231006097K*

DOI: 10.48550/arXiv.2310.06097

TITLE: Discovery of X-ray polarization angle rotation in the jet from blazar Mrk 421.

AUTHOR: Di Gesu, L., Marshall, H. L., Ehlert, S. R., Kim, D. E., Donnarumma, I., Tavecchio, F., Liodakis, I., Kiehlmann, S., Agudo, I., Jorstad, S. G., Muleri, F., Marscher, A. P., Puccetti, S., Middei, R., Perri, M., Pacciani, L., Negro, M., Romani, R. W., Di Marco, A., Blinov, D., Bourbah, I. G., Kontopodis, E., Mandarakas, N., Romanopoulos, S., Skalidis, R., Vervelaki, A., Casadio, C., Escudero, J., Myserlis, I., Gurwell, M. A., Rao, R., Keating, G. K., Kouch, P. M., Lindfors, E., Aceituno, F. J., Bernardos, M. I., Bonnoli, G., Casanova, V., García-Comas, M., Agís-González, B., Husillos, C., Marchini, A., Sota, A., Imazawa, R., Sasada, M., Fukazawa, Y., Kawabata, K. S., Uemura, M., Mizuno, T., Nakaoka, T., Akitaya, H., Savchenko, S. S., Vasilyev, A. A., Gómez, J. L., Antonelli, L. A., Barnouin, T., Bonino, R., Cavazzuti, E., Costamante, L., Chen, C.-T., Cibrario, N., De Rosa, A., Di Pierro, F., Errando, M., Kaaret, P., Karas, V., Krawczynski, H., Lisalda, L., Madejski, G., Malacaria, C., Marin, F., Marinucci, A., Massaro, F., Matt, G., Mitsuishi, I., O'Dell, S. L., Paggi, A., Peirson, A. L., Petrucci, P.-O., Ramsey, B. D., Tennant, A. F., Wu, K., Bachetti, M., Baldini, L., Baumgartner, W. H., Bellazzini, R., Bianchi, S., Bongiorno, S. D., Brez, A., Bucciantini, N., Capitanio, F., Castellano, S., Ciprini, S., Costa, E., Del Monte, E., Di Lalla, N., Doroshenko, V., Dovčiak, M., Enoto, T., Evangelista, Y., Fabiani, S., Ferrazzoli, R., Garcia, J. A., Gunji, S., Hayashida, K., Heyl, J., Iwakiri, W., Kislat, F., Kitaguchi, T., Kolodziejczak, J. J., La Monaca, F., Latronico, L., Maldera, S., Manfreda, A., Ng, C.-Y., Omodei, N., Oppedisano, C., Papitto, A., Pavlov, G. G., Pesce-Rollins, M., Pilia, M., Possenti, A., Poutanen, J., Rankin, J., Ratheesh, A., Roberts, O. J., Sgrò, C., Slane, P., Soffitta, P., Spandre, G., Swartz, D. A., Tamagawa, T., Taverna, R., Tawara, Y., Thomas, N. E., Tombesi, F., Trois, A., Tsygankov, S. S., Turolla, R., Vink, J., Weisskopf, M. C., Xie, F., Zane, S.

PUBLICATION: *Nature Astronomy, 7, 1245-1258*

PUBLICATION DATE: 10/2023

ABSTRACT: *https://ui.adsabs.harvard.edu/abs/2023NatAs...7.1245D*

DOI: 10.1038/s41550-023-02032-7

TITLE: A resolved rotating disk wind from a young T Tauri star in the Bok globule CB 26
AUTHOR: Launhardt, R., Pavlyuchenkov, Y. N., Akimkin, V. V., Dutrey, A., Gueth, F., Guilloteau, S., Henning, T., Piétu, V., Schreyer, K., Semenov, D., Stecklum, B., Bourke, T. L.
PUBLICATION: *Astronomy and Astrophysics, 678, A135*
PUBLICATION DATE: 10/2023
ABSTRACT: *https://ui.adsabs.harvard.edu/abs/2023A&A...678A.135L*
DOI: 10.1051/0004-6361/202347483

TITLE: Linking ice and gas in the Coronet cluster in Corona Australis
AUTHOR: Perotti, G., Jørgensen, J. K., Rocha, W. R. M., Plunkett, A., Artur de la Villarmois, E., Kristensen, L. E., Sewiło, M., Bjerkeli, P., Fraser, H. J., Charnley, S. B.
PUBLICATION: *Astronomy and Astrophysics, 678, A78*
PUBLICATION DATE: 10/2023
ABSTRACT: *https://ui.adsabs.harvard.edu/abs/2023A&A...678A..78P*
DOI: 10.1051/0004-6361/202245541

TITLE: Submillimeter Observations of Magnetic Fields in Massive Star-forming Region W75N
AUTHOR: Zeng, L., Zhang, Q., Alves, F. O., Ching, T.-C., Girart, J. M., Liu, J.
PUBLICATION: *The Astrophysical Journal, 954, 99*
PUBLICATION DATE: 09/2023
ABSTRACT: *https://ui.adsabs.harvard.edu/abs/2023ApJ...954...99Z*
DOI: 10.3847/1538-4357/ace690

TITLE: Protostellar Interferometric Line Survey of the Cygnus-X region (PILS-Cygnus). The role of the external environment in setting the chemistry of protostars
AUTHOR: van der Walt, S. J., Kristensen, L. E., Calcutt, H., Jørgensen, J. K., Garrod, R. T.
PUBLICATION: *Astronomy and Astrophysics, 677, A127*
PUBLICATION DATE: 09/2023
ABSTRACT: *https://ui.adsabs.harvard.edu/abs/2023A&A...677A.127V*
DOI: 10.1051/0004-6361/202245213

TITLE: Precise measurements of self-absorbed rising reverse shock emission from gamma-ray burst 221009A
AUTHOR: Bright, J. S., Rhodes, L., Farah, W., Fender, R., van der Horst, A. J., Leung, J. K., Williams, D. R. A., Anderson, G. E., Atri, P., DeBoer, D. R., Giarratana, S., Green, D. A., Heywood, I., Lenc, E., Murphy, T., Pollak, A. W., Premnath, P. H., Scott, P. F., Sheikh, S. Z., Siemion, A., Titterington, D. J.
PUBLICATION: *Nature Astronomy, 7, 986-995*
PUBLICATION DATE: 08/2023
ABSTRACT: *https://ui.adsabs.harvard.edu/abs/2023NatAs...7..986B*
DOI: 10.1038/s41550-023-01997-9

TITLE: Double SSA spectrum and magnetic field strength of the FSRQ 3C 454.3
AUTHOR: Jeong, H.-W., Lee, S.-S., Cheong, W. Y., Kim, J.-Y., Lee, J. W., Kang, S., Kim, S.-H., Rani, B., Park, J., Gurwell, M. A.
PUBLICATION: *Monthly Notices of the Royal Astronomical Society, 523, 5703-5718*
PUBLICATION DATE: 08/2023
ABSTRACT: *https://ui.adsabs.harvard.edu/abs/2023MNRAS.523.5703J*
DOI: 10.1093/mnras/stad1736

TITLE: Resolving a merger in a hyperluminous submillimeter galaxy at z = 2.82
AUTHOR: Perry, R. W., Chapman, S. C., Smail, I., Bertoldi, F.
PUBLICATION: *Monthly Notices of the Royal Astronomical Society, 523, 2818-2831*
PUBLICATION DATE: 08/2023
ABSTRACT: *https://ui.adsabs.harvard.edu/abs/2023MNRAS.523.2818P*
DOI: 10.1093/mnras/stad1613

TITLE: IXPE and Multiwavelength Observations of Blazar PG 1553+113 Reveal an Orphan Optical Polarization Swing
AUTHOR: Middei, R., Perri, M., Puccetti, S., Liodakis, I., Di Gesu, L., Marscher, A. P., Rodriguez Cavero, N., Tavecchio, F., Donnarumma, I., Laurenti, M., Jorstad, S. G., Agudo, I., Marshall, H. L., Pacciani, L., Kim, D. E., Aceituno, F. J., Bonnoli, G., Casanova, V., Agís-González, B., Sota, A., Casadio, C., Escudero, J., Myserlis, I., Sievers, A., Kouch, P. M., Lindfors, E., Gurwell, M., Keating, G. K., Rao, R., Kang, S., Lee, S.-S., Kim, S.-H., Cheong, W. Y., Jeong, H.-W., Angelakis, E., Kraus, A., Antonelli, L. A., Bachetti, M., Baldini, L., Baumgartner, W. H., Bellazzini, R., Bianchi, S., Bongiorno, S. D., Bonino, R., Brez, A., Bucciantini, N., Capitanio, F., Castellano, S., Cavazzuti, E., Chen, C.-T., Ciprini, S., Costa, E., De Rosa, A., Del Monte, E., Di Lalla, N., Di Marco, A., Doroshenko, V., Dovčiak, M., Ehlert, S. R., Enoto, T., Evangelista, Y., Fabiani, S., Ferrazzoli, R., García, J. A., Gunji, S., Hayashida, K., Heyl, J., Iwakiri, W., Kaaret, P., Karas, V., Kislat, F., Kitaguchi, T., Kolodziejczak, J. J., Krawczynski, H., La Monaca, F., Latronico, L., Maldera, S., Manfreda, A., Marin, F., Marinucci, A., Massaro, F., Matt, G., Mitsuishi, I., Mizuno, T., Muleri, F., Negro, M., Ng, C.-Y., O'Dell, S. L., Omodei, N., Oppedisano, C., Papitto, A., Pavlov, G. G., Peirson, A. L., Pesce-Rollins, M., Petrucci, P.-O., Pilia, M., Possenti, A., Poutanen, J., Ramsey, B. D., Rankin, J., Ratheesh, A., Roberts, O. J., Romani, R. W., Sgrò, C., Slane, P., Soffitta, P., Spandre, G., Swartz, D. A., Tamagawa, T., Taverna, R., Tawara, Y., Tennant, A. F., Thomas, N. E., Tombesi, F., Trois, A., Tsygankov, S. S., Turolla, R., Vink, J., Weisskopf, M. C., Wu, K., Xie, F., Zane, S.
PUBLICATION: *The Astrophysical Journal, 953, L28*
PUBLICATION DATE: 08/2023
ABSTRACT: *https://ui.adsabs.harvard.edu/abs/2023ApJ...953L..28M*
DOI: 10.3847/2041-8213/acec3e

TITLE: Detection of a High-velocity Jet from MWC 349A Traced by Hydrogen Recombination Line Maser Emission
AUTHOR: Prasad, S., Zhang, Q., Moran, J., Cao, Y., Jimenéz-Serra, I., Martín-Pintado, J., Martínez-Henares, A., Báez-Rubio, A.
PUBLICATION: *The Astrophysical Journal, 953, L6*
PUBLICATION DATE: 08/2023
ABSTRACT: *https://ui.adsabs.harvard.edu/abs/2023ApJ...953L...6P*
DOI: 10.3847/2041-8213/ace7ba

TITLE: Testing the Linear Relationship between Black Hole Mass and Variability Timescale in Low-luminosity AGNs at Submillimeter Wavelengths
AUTHOR: Chen, B.-Y., Bower, G. C., Dexter, J., Markoff, S., Ridenour, A., Gurwell, M. A., Rao, R., Wallström, S. H. J.
PUBLICATION: *The Astrophysical Journal, 951, 93*
PUBLICATION DATE: 07/2023
ABSTRACT: *https://ui.adsabs.harvard.edu/abs/2023ApJ...951...93C*
DOI: 10.3847/1538-4357/acd250

Photo by Brooks Rownd

The Submillimeter Array (SMA) is a pioneering radio-interferometer dedicated to a broad range of astronomical studies including finding protostellar disks and outflows; evolved stars; the Galactic Center and AGN; normal and luminous galaxies; and the solar system. Located on Maunakea, Hawaii, the SMA is a collaboration between the Smithsonian Astrophysical Observatory and the Academia Sinica Institute of Astronomy and Astrophysics.

SUBMILLIMETER ARRAY
Center for Astrophysics | Harvard & Smithsonian
60 Garden Street, MS 78
Cambridge, MA 02138 USA
www.cfa.harvard.edu/sma/

SMA HILO OFFICE
645 North A'ohoku Place
Hilo, Hawaii 96720
Ph. 808.961.2920
Fx. 808.961.2921
sma1.sma.hawaii.edu

ACADEMIA SINICA INSTITUTE
OF ASTRONOMY & ASTROPHYSICS
11F of Astronomy-Mathematics Building,
AS/NTU, No. 1, Sec. 4, Roosevelt Road
Taipei 10617
Taiwan R.O.C.
www.asiaa.sinica.edu.tw/